

SKB

**TECHNICAL
REPORT**

88-02**Migration of the fission products
strontium, technetium, iodine, cesium
and the actinides neptunium, plutonium,
americium in granitic rock**Thomas Ittner¹, Börje Torstenfelt¹ and Bert Allard²¹ Department of Nuclear Chemistry
Chalmers University of Technology
Göteborg, Sweden² Department of Water in Environment and Society
University of Linköping,
Linköping, Sweden

Januari 1988

SVENSK KÄRNBRÄNSLEHANTERING AB*SWEDISH NUCLEAR FUEL AND WASTE MANAGEMENT CO*

BOX 5864 S-102 48 STOCKHOLM

TEL 08-665 28 00 TELEX 13108-SKB

MIGRATION OF THE FISSION PRODUCTS STRONTIUM, TECHNETIUM,
IODINE, CESIUM AND THE ACTINIDES NEPTUNIUM, PLUTONIUM,
AMERICIUM IN GRANITIC ROCK

Thomas Ittner¹, Börje Torstenfelt¹ and Bert Allard²

1 Department of Nuclear Chemistry
Chalmers University of Technology
Göteborg, Sweden

2 Department of Water in Environment and Society
University of Linköping
Linköping, Sweden

January 1988

This report concerns a study which was conducted for SKB. The conclusions and viewpoints presented in the report are those of the author(s) and do not necessarily coincide with those of the client.

Information on KBS technical reports from 1977-1978 (TR 121), 1979 (TR 79-28), 1980 (TR 80-26), 1981 (TR 81-17), 1982 (TR 82-28), 1983 (TR 83-77), 1984 (TR 85-01), 1985 (TR 85-20), 1986 (TR 86-31) and 1987 (TR87-33) is available through SKB.

*
MIGRATION OF THE FISSION PRODUCTS
STRONTIUM, TECHNETIUM, IODINE, CESIUM
AND THE ACTINIDES
NEPTUNIUM, PLUTONIUM, AMERICIUM
IN GRANITIC ROCK

Thomas Ittner*, Börje Torstenfelt* and Bert Allard**

*Department of Nuclear Chemistry,
Chalmers University of Technology,
S-412 96 Göteborg, Sweden.

**Department of Water in Environment and Society,
University of Linköping,
S-581 83 Linköping, Sweden.

1988-01-21

CONTENTS

	Page
SUMMARY	1
1. INTRODUCTION	2
2. EXPERIMENTAL	2
2.1. Radionuclides	2
2.2. Migration measurements	3
2.2.1. Diffusion measurements	3
2.2.2. Autoradiography	3
2.3. Rocks	4
2.4. Groundwater chemistry	8
2.5. Experimental conditions	8
3. DIFFUSION THEORY	8
4. RESULTS AND DISCUSSION	11
4.1. Fission products	11
4.1.1. Strontium	14
4.1.2. Technetium	14
4.1.3. Iodine	14
4.1.4. Cesium	15
4.2. Actinides	16
4.2.1. Neptunium	16
4.2.2. Plutonium	16
4.2.3. Americium	17
5. CONCLUSIONS	17
6. ACKNOWLEDGEMENTS	18
7. REFERENCES	18
APPENDIX	21

SUMMARY

The migration of the fission products strontium, technetium, iodine and cesium and the actinides neptunium, plutonium and americium in granitic rock has been studied.

Rock samples were taken from drilling cores in granitic and granodioritic rock, and small (2x2x2 cm) rock tablets from the drilling cores were exposed to a groundwater solution containing one of the studied elements at trace levels. The concentration of the element versus penetration depth in the rock tablet was measured radiometrically. The sorption on the mineral faces and the migration into the rock was studied, by an autoradiographic technique.

The cationic fission products strontium and cesium had apparent diffusivities of 10^{-13} - 10^{-14} m²/s. They migrate mainly in fissures or filled fractures containing e.g., calcite, epidote or chlorite or in veins with high capacity minerals (e.g. biotite).

The anionic fission products iodine and technetium had apparent diffusivities of about 10^{-14} m²/s. These species migrate along mineral boundaries and in open fractures and to a minor extent in high capacity mineral veins.

The migration of the actinides neptunium, plutonium and americium is very slow (in the mm-range after 2-3 years contact time). The apparent diffusivities were about 10^{-15} m²/s. The actinide migration into the rock was largely confined to fissures.

1. INTRODUCTION

One of the main factors governing the long-term safety of an underground repository for the high level radioactive waste, is the transport path-ways through the bedrock to the biosphere, ones the radionuclides have been released into the groundwater.

The chemical composition of the groundwater and the groundwater flow would have a large influence on the mobility of the radionuclides. Also the mineralogy of the rock, the number of fissures and their apertures, the frequency of microfissures, and the composition of fracture minerals and weathering products covering the fissure walls would influence the transport of the radionuclides through the rock.

The fracture minerals and the weathering products covering the fracture surfaces normally have higher sorption capacities than the underlying rock itself. Thus, the fracture coating minerals would increase the sorption of cesium, technetium and americium, as compared to the sorption on the bedrock (Allard et al 1982a).

In this study, diffusion of the fission products strontium, technetium, iodine and cesium and the actinides neptunium, plutonium and americium into polished and weathered rock samples has been measured. The method has been previously described (Allard et al, 1985), and results have been published. (Ittner et al 1988a; Ittner et al 1988b)

2. EXPERIMENTAL

2.1. Radionuclides

The fission products in this study were strontium, technetium, iodine and cesium. Cesium and strontium, as Cs-137 and Sr-90, are two of the dominating radionuclides in the nuclear high-level waste during the first 500 years after the discharge from the reactor. They can be considered as model elements for mono- and divalent non-hydrolysed cations, respectively. They both exhibit a significant sorption on granite (Torstenfelt 1982a). Technetium-99 and iodine-129 are long-lived radionuclides which contribute to the long-term hazard of the waste. Technetium is hepta valent and anionic under oxidizing

conditions (as pertechnetate, TcO_4^-) and has little tendency to be sorbed on the rock. Under reducing conditions technetium would be tetravalent and at neutral pH hydrolyzed (as TcO_2 or Tc(OH)_4) and is sorbing on the rock (Allard et al, 1979). Iodine is anionic and is not expected to interact with the solid.

The actinides used in this study were neptunium, plutonium and americium. They are all long-lived alpha-emitters and contribute to the long-term hazard of the waste. Neptunium is pentavalent (as NpO_2^+) and not hydrolyzed at pH below 8-9. Plutonium is probably tetravalent and americium is trivalent, in most groundwaters (Allard et al, 1982b). At neutral pH, both plutonium and americium are highly hydrolyzed and show a high surface sorption.

2.2. Migration measurements

2.2.1. Diffusion experiments

Rock samples were sawn into small rock tablets (2x2x2 cm). The tablets were covered with a thin resin on all sides except for one and then submerged into synthetic groundwater spiked with a radioactive trace element. After a contact time of three months up to three years the rock was taken up of the spiked solution and washed. Successive 0.05-0.1 mm thick layers of the rock tablet were removed by grinding. The trace element was analyzed radiometrically, giving a concentration profile (concentration vs. penetration depth) of the element in the rock.

2.2.2. Autoradiography

The autoradiographic study shows in which path-ways the trace element is migrating, and by comparing with photographs of the surfaces it is possible to distinguish if the migration is through small fissures or if it is through minerals or mineral boundaries. Autoradiographs were taken on the rock surface after each grinding. The rock sample was covered with a thin plastic film and put on a photographic film for exposure for 7 hours up till 10 days, depending on the radionuclide and its concentration on the rock surface. Every rock sample had its own individual photographic exposure time. This exposure time was extended at the end of the autoradiographic series in order to get better information about low concentrations of the radionuclide in the rock matrix.

2.3. Rocks

The rock samples were taken from drilling cores at various depths at Finnsjön and Studsvik and from stuffs in the Stripa mine. Samples were taken either along a major fracture surface, or from intact rock free from major fractures. The surface of these coupons were polished. The mineralogic composition of the rock samples used in the fission product experiments and the actinide experiments are listed in Table 1 and 2, respectively.

The Finnsjön rock is a foliated granodiorit with colour varying from grey to greyish red. The grains are of medium size (Ahlbom et al, 1986). The red color is due to a precambrian hematitisation of hydrothermal origin. The average mineral content expressed as volume percent of the granodiorit is 32% plagioclase, 30% quartz, 18% microcline, 11% hornblende, 9% biotite and chlorite. Minor amounts of epidote, apatite, titanite and sericite are frequent.

The rock from Studsvik is a gneiss of sedimentary origin which in part is strongly migmatized and veined. It is characterized as a very heterogeneous rock with biotite-foliated paleosoms. Typical minerals in the paleosoms are quartz 40-70%, feldspars 10-40%, biotite and chlorite. Andalusite, sillimanite, garnet and cordierite are minerals which usually constitute up to 20% of the paleosoms. Garnet as well as cordierite is also present in neosomes (Tullborg et al, 1982).

The rock from Stripa is a gray to redish medium grained homogeneous granite. The red color is due to hematite. The Stripa granite contains 30-40% microcline and 5-10% biotite and chlorite. The hematite is in some places dispersed as a fine dust within feldspar grains, particularly in plagioclase, or along grain boundaries and cracks within the grains. Fractures are frequent both continuous and discontinuous on a microscopic scale. Fine discontinuous cracks within primary grains or along grain boundaries are common, even in relatively unfractured rock. These cracks are filled with intergrown chlorite and sericite or by quartz and feldspars and they frequently originate from primary grains of the same minerals as those filling the cracks. (Wollenberg et al, 1980; Nordstrom et al, 1986)

Table 1

Mineralogical composition of the rock samples used in the diffusivity measurements of the fission products. (qz = quartz, pl = plagioclase, mi = microcline, or = orthoclase, bi = biotite, ch = chlorite, ga = garnet, mu = muscovite, ho = hornblende, ep = epidote, ca = calcite, pr = prehnite, la = laumontite, pa = palygorskite, sm = smectite, mb = microbreccia with calcite, epidote, muscovite and chlorite healing, mc = microbreccia with epidote, chlorite and muscovite healing).

Sample	Element	Fracture ^a	Mineralogy ^b	Sampling location	
Fi7 526.5	⁹⁰ Sr	no	p qz pl mi bi	Finnsjön	
Str 2:2		yes	p qz mi pl bi ch	Stripa	
Stu 6:3		no	p qz pl ga bi	Studsvik	
Fi6 309.0:4	⁹⁹ Tc	no	w ca	Finnsjön	
Fi7 318.8:4		no	w qz mi bi ch ca	Finnsjön	
Fi7 526.5:4r		no	p qz or pl bi	Finnsjön	
Fi8 72.0:3	¹²⁵ I	no	w ca qz pr la	Finnsjön	
Fi8 134.8:3		(yes),qz	w ca la ch	Finnsjön	
Stu 29.3:3		no	w ca qz ch ga (bi)	Studsvik	
Str A:3N		(yes),ch	w ca ep ch qz mi (bi)	Stripa	
Str 1:5		(yes),qz	w qz pl mi mc	Stripa	
Fi B:2		yes	p qz bi pl (greenish)	Finnsjön	
Str 2:1		yes	p qz mi pl bi	Stripa	
Stu A:2		no	p qz pl ga bi	Studsvik	
Fi6 309.0:1		¹³⁷ Cs	no	w ca (pr)	Finnsjön
Fi7 318.8:1			(yes)	w qz mi bi ch ca	Finnsjön
Fi7 526.5:2r	no		w qz mi pl bi	Finnsjön	
Fi8 72.0:1	yes		w ca qz pr la	Finnsjön	
Fi8 358.1:1	no		w ca la (pr) he	Finnsjön	
Stu 5.4:1	yes		w ca qz (bi pa)	Studsvik	
Stu 104.2	no		w sm (ca qz)	Studsvik	
Stu 183.1:1	(yes)		w ca qz ga (bi)	Studsvik	
Str A:1vr	(yes),ch	p qz pl mi mu ho	Stripa		
Str A:1N	(yes)	w ca ep cl qz mi (bi)	Stripa		
Str MS:2	yes	w qz pl mi mb	Stripa		
Str 1:1	yes	w qz pl mi mc	Stripa		

^aContaining a minor fracture (open or sealed) "perpendicular" to the sample surface. ^bAt sample surface; p = polished surface, w = weathered surface (mainly fracture minerals).

Table 2

Mineralogical composition of the rock samples used in the diffusivity measurements of the actinides. (qz = quartz, pl = plagioclase, bi = biotite, he = hematitised, ch = chlorite, mi = microcline, ho = hornblende, ca = calcite, pr = prehnite, la = laumontite, cm = claymineral, mb = microbreccia with calcite, epidote, muscovite and chlorite healing).

Sample	Element	Fracture ^a	Mineralogy ^b	Sampling location
Fi8 358,1:1	²³⁷ Np	yes,ca	p qz pl bi he	Finnsjön
Str 3:4		yes	p qz pl bi ch	Stripa
Fi8 358,1:2	²³⁹ Pu	yes,la	p qz pl bi he	Finnsjön
Str 4:2		no	p qz pl mi bi	Stripa
Str 4:1		yes	p qz pl mi bi	Stripa
Fi6 309.0:3	²⁴¹ Am	no	w ca (pr)	Finnsjön
Fi7 526.5:3		no	w ca la cm ch (pr)	Finnsjön
Fi8 358,1:3		yes,ca	p qz pl bi he	Finnsjön
Stu 183.1:1r		no	p qz pl ho bi	Studsвик
Str 3:1		yes	p qz pl bi ch	Stripa
Str MS:3		no	w qz pl mi mb	Stripa

^aContaining a minor fracture (open or sealed) "perpendicular" to the sample surface.

^bAt sample surface; p = polished surface, w = weathered surface (mainly fracture minerals).

Table 3

Chemical composition (mg/l) of the synthetic groundwaters representative of the groundwaters from the rock sampling locations (Hultberg et al, 1981; Landström et al, 1982; Laurent 1982; Allard et al, 1983)

Species	Origin				
	Str	Stu	Fi6	Fi7	Fi8
Na ⁺	49	90	959	274	320
K ⁺	0.59	2.8	16	16	12
Ca ²⁺	14	31	554	134	37
Mg ²⁺	0.23	9	69	16	12
HCO ₃ ⁻	86	195	123	280	263
NO ₃ ⁻			6		2.0
F ⁻			1	1.8	2.3
Cl ⁻	35	57	2407	477	387
SO ₄ ²⁻	4.9	36	205	45	42
SiO ₂ (total)	5.5	11	17	13	12
pH	8.9	7.3	7.7	8.1	8.3

Str = Stripa; Stu = Studsvik; Fi = Finnsjön

2.4. Groundwater Chemistry

The aqueous phases used in the laboratory tests were synthetic groundwaters (Table 3). They represent the waters sampled in the drilling holes at Finnsjön, Studsvik and in the Stripa mine, at the same depths as the origin of the solid rock samples.

2.5. Experimental conditions

The experimental conditions are given in Table 4 (cf. Allard et al, 1985). The total volume of synthetic groundwater in each system was 25 ml. A magnetic stirrer was used in order to keep a uniform concentration in the solution. The grinding procedure has previously been described by Andersson et al (1981). The radioactivity was measured directly on the rock surface (e.g., by using a NaI-detector or a ZnS-detector).

3. DIFFUSION THEORY

Diffusion of a trace element through a porous solid is dependent on molecular diffusion in the aqueous phase, sorption phenomena on the solid, and on the pore constrictivity and tortuosity of the solid. Thus, the measured diffusivity in experiments of the present kind would be the apparent diffusivity, D_a , and not the molecular diffusivity, D .

The apparent diffusivity for one-dimensional diffusion is given by

$$\frac{dC}{dt} = \frac{d}{dx} \left(D_a \frac{dC}{dx} \right) \quad (1)$$

The analytical solution for the case with a linear sorption isotherm and constant concentration in the solution during the experiment is (Crank 1975):

$$\frac{C}{C_0} = \operatorname{erfc} \left(\frac{x}{2\sqrt{D_a t}} \right) \quad (2)$$

Table 4

Experimental conditions (Fi = Finnsjön, Str = Stripa, Stu = Studsvik)

Sample	Nuclide	Contact time ^a (days)	Water ^b	pH ^c	C ^d (M)	
Fi7 526.5	⁹⁰ Sr	164	Fi7		10 ⁻⁷	
Str 2:2		432	Str	8.3	10 ⁻⁷	
Stu 6:3		657	Stu	8.5	10 ⁻⁷	
Fi6 309.0:4	⁹⁹ Tc	349	Fi6		10 ⁻⁶	
Fi7 318.8:4		349	Fi7		10 ⁻⁶	
Fi7 526.5:4r		85	Fi7		10 ⁻⁶	
Fi8 72.0:3		167	Fi8		10 ⁻⁶	
Fi8 134.8:3		349	Fi8		10 ⁻⁶	
Stu 29.3:3		167	Stu		10 ⁻⁶	
Str A:3N		257	Str		10 ⁻⁶	
Str 1:5		167	Str		10 ⁻⁶	
Fi B:2		¹²⁵ I	153	Fi8		10 ⁻⁵
Str 2:1			421	Str	7.7	10 ⁻⁵
Stu A:2	421		Stu	8.0	10 ⁻⁵	
Fi6 309.0:1	¹³⁷ Cs	167	Fi6		10 ⁻⁶	
Fi7 318.8:1		132	Fi7		10 ⁻⁶	
Fi7 526.5:2r		357	Fi7		10 ⁻⁶	
Fi8 72.0:1		167	Fi8		10 ⁻⁶	
Fi8 358.1:1		265	Fi8		10 ⁻⁶	
Stu 5.4:1		132	Stu		10 ⁻⁶	
Stu 104.2		167	Stu		10 ⁻⁶	
Stu 183.1:1		265	Stu		10 ⁻⁶	
Str A:1vr		85	Str		10 ⁻⁶	
Str A:1N		167	Str		10 ⁻⁶	
Str MS:2		167	Str		10 ⁻⁶	
Str 1:1		132	Str		10 ⁻⁶	

^aDays the rock sample was in contact with the spiked groundwater solution.

^bThe composition of the groundwater solution is given in Table 1.

^cpH in the solution at the end of the experiment.

^dRadionuclide concentration in solution at the start of the migration experiments.

Table 4, Continued

Experimental conditions (Fi = Finnsjön, Str = Stripa, Stu = Studsvik)

Sample	Nuclide	Contact time ^a (days)	Water ^b	pH ^c	C ^d (M)
Fi8 358.1:1	²³⁷ Np	866	Fi8	8.4	10 ⁻⁸
Str 3:4		654	Str	8.4	10 ⁻⁸
Fi8 358.1:2	²³⁹ Pu	854	Fi8	4.1	10 ⁻⁹
Str 4:2		858	Str	2.9	10 ⁻⁹
Str 4:1		646	Str	3.0	10 ⁻⁹
Fi6 309.0:3	²⁴¹ Am	355	Fi6		10 ⁻⁸
Fi7 526.5:3		263	Fi7		10 ⁻⁸
Fi8 358.1:3		877	Fi8	8.4	10 ⁻⁹
Stu 183.1:1r		85	Stu		10 ⁻⁸
Str 3:1		665	Str	8.6	10 ⁻⁹
Str MS:3		1202	Str	8.9	10 ⁻⁹

^aDays the rock sample was in contact with the spiked groundwater solution.^bThe composition of the groundwater solution is given in Table 1.^cpH in the solution at the end of the experiment.^dRadionuclide concentration in solution at the start of the migration experiments.

where C = the concentration (mol/m^3) in the pore water at distance x and time t , C_0 = the constant concentration (mol/m^3) in the pore water in the first thin layer at the surface of the solid, x = the distance from the surface (m), t = the diffusion time (s), and erfc = the error function complement ($=1-\text{erf}$). The diffusivity is evaluated from eqn (2). When z in $\text{erfc}(z)$ is plotted against x , the slope of the line gives D_a from $z = x/2\sqrt{D_a t}$ where t is known. In Figures 1 to 37 data are given for r^2 , a , b and D_a , where a is the intersection with the y -axis, b is the slope of the line from the linear equation, $y = ax + b$, and r^2 is the correlation coefficient of the fit of the data to the equation.

The apparent diffusivity in rock would be lower in rock under natural stress conditions than in laboratory samples due to compression. Skagius et al (1985) found in laboratory stress experiments that the diffusivity was reduced 20 to 70 percent in the samples under 300 to 350 bars pressure, compared to samples under atmospheric pressure. Birgersson et al (1983) found no change in apparent diffusivity in field measurements in the Stripa mine compared to laboratory measurements.

4. RESULTS AND DISCUSSION

The results of the diffusion measurements are given in Table 5 and Figures 1 to 37, autoradiographs in Figures 38 - 54 and calculated diffusivities in table 5. In the figures the plotted curve sometimes starts at a certain distance into the sample or the first experimental values are not used in the evaluation. The surfaces of these rock coupons are rough and have to be ground completely planar before a mathematical treatment of the diffusion profile can be done.

4.1. Fission products

In figures 1 - 26 the curves for z in $\text{erfc}(z)$ versus the depth x are given for the fission products technetium, strontium, iodine and cesium.

Table 5.

Measured apparent diffusivities.

Sample	Nuclide	D_a	10^{14}	(m^2/s)	
Fi7 526.5	^{90}Sr	49			
Str 2:2		2.7			
Stu 6:3		2.4			
Fi6 309.0:4	^{99}Tc	30			
Fi7 318.8:4		1.9			
Fi7 526.5:4r		(4.5)			
Fi8 72.0:3		11			
Fi8 134.8:3		2.2			
Stu 29.3:3		2.2			
Str A:3N		(20.5)			
Str 1:5		2.2			
Fi B:2		^{125}I	1.9		
Str 2:1			3.2	(0.028) ^a	
Stu A:2	1.5		(0.021) ^a		
Fi6 309.0:1	^{137}Cs	500			
Fi7 318.8:1		12	(110) ^a		
Fi7 526.5:2r		22			
Fi8 72.0:1		8.3			
Fi8 358.1:1		14			
Stu 5.4:1		5.9			
Stu 104.2		3.5			
Stu 183.1:1		11			
Str A:1vr		18	(140) ^a		
Str A:1N		2.4	(30) ^a		
Str MS:2		3.4			
Str 1:1		2.5	(37) ^a		

^a Possibly two species (or mechanisms); cf. figures.

Table 5., continued.
 Measured apparent diffusivities.

Sample	Nuclide	$D_a \cdot 10^{14}$ (m ² /s)
Fi8 358.1:1	²³⁷ Np	0.33
Str 3:4		0.41
Fi8 358.1:2	²³⁹ Pu	0.16
Str 4:2		0.12
Str 4:1	²⁴¹ Am	0.15 (1.5) ^a
Fi6 309.0:3		2.3
Fi7 526.5:3		2.8
Fi8 358.1:3		0.039
Stu 183.1:1r		0.071
Str 3:1		0.10
Str MS:3		0.38

^a Possibly two species (or mechanisms); cf. figures.

4.1.1 Strontium

The apparent diffusivity of strontium was 4.9×10^{-13} , 2.7×10^{-14} and 2.4×10^{-14} m^2/s for the Finnsjö, Stripa and Studsvik rocks, respectively. Strontium migrated into the rock mainly through veins of high-capacity minerals such as biotite, chlorite and hornblende. Small open fissures or fissures filled with clayish material also acted as transport channels into the rock. The sorption on the rock surface were selective. High-capacity minerals such as biotite and chlorite were good sorbents, while the feldspars and particularly quartz were poor sorbents.

From sample Str 2:2 it appears that biotite grains constitute the main strontium sorbents as well as the major transport channels into the rock. A biotite grain 1.72 mm below the surface is blackened to the same magnitude as grains the surface. However, another biotite grain, situated at surface, is hardly blackened at all, this could possibly be due to the sheet structure of biotite. Chlorite has sometimes a weak blackening and sometimes blackening at the mineral edges. These chlorite grains seem to be transformed biotite. There is no obvious reason why the diffusivity for the Finnsjö samples is about 20 times higher than for the others.

4.1.2. Technetium

The apparent diffusivity of technetium in granite was usually around 2×10^{-14} m^2/s . A comparatively high diffusion (3.0×10^{-13} m^2/s) is observed in the calcite mineral (Fig. 4, Fi6 309.0:4), and in the laumontite/ prehnite mineral (1.1×10^{-13} m^2/s ; Fig. 7, Fi8 72.0:3). The value measured in sample Str A:3N of the Stripa granite (Fig. 10) is probably somewhat high due to the very rough surface of the coupon at the start of the experiment.

The migration of technetium in granite was, according to the autoradiographic study, confined to grain boundaries and fissures. Technetium was not sorbed on any particular mineral.

4.1.3 Iodine

The apparent diffusivity of iodine (as iodide) was 1.9×10^{-14} , 3.2×10^{-14} and 1.5×10^{-14} m^2/s for the Finnsjö, Stripa and Studsvik rocks, respectively. The migration of iodine into the rock was not associated with any particular

mineral. The surface sorption showed a tendency to be higher on biotite, but otherwise no significant differences were observed for the various minerals. The sorption on biotite could be due to the sheet structure of the micas, leading to diffusion of iodide into the biotite when the sheet structure are perpendicular to the surface of the rock tablet. The autoradiographs on the Studsvik gneiss (e.g. Fig. 14, Stu A:2) show a slight accumulation in the grain boundaries between the minerals.

Similar to what was observed for the diffusion of iodine in clay (Torstenfelt, 1986a), it seems that the iodine diffuses through two mechanisms (cf., Figs. 13 and 14), possibly due to different species of the iodine.

4.1.4. Cesium

The apparent diffusivity of cesium in the granites varied in the range 2×10^{-14} to 10^{-12} m²/s. For some of the samples two mechanisms were indicated, just as for iodine, with diffusivities in the range $(3 \text{ to } 14) \times 10^{-13}$ m²/s and $(2 \text{ to } 18) \times 10^{-14}$ m²/s, respectively. The diffusivity in a sample with a calcite healed fracture (Fig. 15, Fi6 309.0:1) was as high as 5.0×10^{-12} m²/s. Similar values have previously been observed (Torstenfelt et al, 1982a).

The migration of cesium into the rock was mainly occurring in high-capacity mineral veins (biotite, chlorite, hornblende etc.) and also in fissures and fractures sealed with high-capacity minerals such as chlorite and epidote. The major sorption mechanism for cesium, which is a monovalent cation, is cation exchange. The sorption on high-capacity minerals and most weathering products is accordingly high (Allard et al, 1982a; Torstenfelt et al 1982b). Most of the present rock samples, had weathered surfaces, with a high cation exchange capacities leading to a pronounced cesium sorption on these fracture surfaces.

This means that a weathered rock surface, due to high sorption on the surface and enhanced transport through the weathered layer into the underlying fresh rock would increase the removal of cesium from the water phase, as compared to a fresh rock surface.

4.2 Actinides

In figures 27 - 37 the curves for z in $\text{erfc}(z)$ versus the diffusion distance x is given for the actinides neptunium, plutonium and americium.

4.2.1. Neptunium

The apparent diffusivity of neptunium in Finnsjön and Stripa granite was 3.3×10^{-15} and 4.1×10^{-15} m^2/s , respectively. The autoradiographs showed a selective sorption pattern of neptunium, with a somewhat higher sorption on biotite than on the feldspars and quartz. The diffusion of neptunium into the rock is slow. At a depth of 1 millimeter no more neptunium could be detected. In the two samples (Figs. 27 and 28, Fi8 358.1:1 and Str 3:4) the diffusion in one fissure was extending beyond the gross penetration depth of the neptunium, indicating that the transport of neptunium is mainly confined to open pores and microfissures of the rock.

Even though neptunium was sorbed mostly on high-capacity minerals, the dependence of these minerals as transport path-ways into the rock was much less pronounced as compared to what was observed for cesium and strontium. This is due to the predominantly physical adsorption of the actinides (due to the hydrolysis, Allard et al, 1982b) as compared to the cation exchange sorption of cesium and strontium.

4.2.2. Plutonium

The apparent diffusivity of plutonium was 1.7×10^{-15} m^2/s in the Finnsjö granite, and in the range $(1.2 - 1.5) \times 10^{-15}$ m^2/s in the Stripa granite. Plutonium showed a similar sorption behaviour as neptunium. However the diffusion into the biotite seemed to be more pronounced and possibly also the migration into open fissures (cf., Fig 31, Str 4:1). In the laumontite healed fracture (Fig. 29, Fi8 358,1:2) no penetration into the rock was observed.

Plutonium seemed to migrate with more than one mechanism (cf., Fig. 31). This could be due to the complicated redox chemistry of plutonium, where more than one oxidation state can exist in solution at the same time. Thus, the total measured diffusion profile in the rock could consist of overlapping diffusion profiles from two or more different plutonium species. The same effect is observed for the diffusion of redox sensitive actinides in clay (Torstenfelt,

1986b). However, in Str 4:2 (fig 31) there is evidently a fissure which is the major path-way into the rock leading to a fraction with higher velocity. In the plutonium system pH was low (3-4). At a higher pH the sorption of plutonium (presumably as Pu(IV)) would be higher, giving an even lower diffusivity.

4.2.3. Americium

The apparent diffusivity of americium in polished granite was in the range $(0.4 - 4) \times 10^{-15} \text{ m}^2/\text{s}$. Americium exhibited a very high surface sorption regardless of the minerals, although more americium was sorbed on biotite than on the feldspars and quartz. The penetration into unfractured rock seemed to be very small (almost zero), but open fractures was one possible transport path for americium in the rock (cf., Fig 53, Str 3:1). The calculated diffusivities into the rocks with a weathered surface (Fig. 33, Fi7 526.5:3) was at least one order of magnitude higher than in polished granite samples. However, the high value for Fi6 309.0:3 could possibly also be related to the presence of calcite.

5. CONCLUSIONS

The fission products cesium and strontium, which are mono- and divalent cations respectively, both migrate into the rock in high-capacity mineral veins, through open fractures or through closed fractures sealed with minerals such as chlorite, epidote and calcite. In fractures leached with quartz no migration could be observed. The apparent diffusivities were $(2 - 20) \times 10^{-14} \text{ m}^2/\text{s}$ and $(2 - 3) \times 10^{-14} \text{ m}^2/\text{s}$, respectively, in polished granite without open fractures.

The fission products technetium and iodine are negatively charged ions, technetium as pertechnetate, TcO_4^- , and iodine as iodide, I^- . The apparent diffusivities for technetium and iodine are $(2 - 3) \times 10^{-14} \text{ m}^2/\text{s}$, which are low considering that these species sorb very poorly on the minerals. The diffusion is, in fact, slower than for the sorbing cesium. This could be due to steric effects for the anions, which are confined to transport mainly in grain boundaries or through open fractures, and probably to a much lesser content in the high-capacity minerals.

The actinides neptunium, plutonium and americium are highly hydrolyzed. In the polished samples of fresh granites without any open fractures the

apparent diffusivities are around $(3 - 4) \times 10^{-15} \text{ m}^2/\text{s}$, $(1 - 2) \times 10^{-15} \text{ m}^2/\text{s}$ and $(0.4 - 1) \times 10^{-15} \text{ m}^2/\text{s}$ for neptunium, plutonium and americium, respectively. They have an overall high surface sorption, with comparatively lower sorption on quartz and the feldspars and higher sorption on the dark minerals, like biotite and hornblende. For americium the sorption is more uniformly distributed. This is in accordance with the sorption behaviour observed in e.g. batch studies on pure minerals (Allard et al, 1982b). The migration into the rock is largely occurring in fissures. Near-surface migration (mm range) is also dependent on small open fissures.

6. ACKNOWLEDGEMENTS

The experimental help by Ms. Lena Eliasson and Ms. Wanda Johansson, as well as help with the preparation of the figures by Ms. Lena Eliasson are gratefully acknowledged. We would also like to thank Dr Erik Ehn, CEA, Strängnäs, Sweden, for help with finding film suitable for the autoradiographs. This work was financed by SKB, Division KBS.

7. REFERENCES

Ahlbom, K., Andersson, P., Ekman, L., Gustafsson, E., Smellie, J., Tullborg, E.-L: Preliminary Investigations of Fracture Zones in the Brädan area, Finnsjön Study Site, SKB TR 86-05, SKB, Stockholm 1986.

Allard, B., Kipatsi, H., Torstenfelt, B: Technetium: Reduction and Sorption in Granitic Bedrock, *Radiochem. Radioanal. Letters* 37(4-5) (1979) 223-230.

Allard, B., Larson, S.-A., Albinsson, Y., Tullborg, E.-L., Karlsson, M., Andersson, K., Torstenfelt, B: Minerals and Precipitates in Fractures and Their Effects on the Retention of Radionuclides in Crystalline Rock, Proc. Workshop on Near-Field Phenomena in Geologic Repositories for Radioactive Waste, OECD/NEA, Paris 1982a, pp. 93-100.

Allard, B., Olofsson, U., Torstenfelt, B., Kipatsi, H., Andersson, K: Sorption of Actinides in Well-Defined Oxidation States on Geologic Media, in W. Lutze (Ed.), Scientific Basis for Nuclear Waste Management - V, Elsevier, New York 1982b, pp. 775-782.

Allard, B., Larson, S.-A., Tullborg, E.-L., Wikberg, P: Chemistry of Deep Groundwaters From Granitic Bedrock, SKBF/KBS TR 83-59, SKB, Stockholm 1983.

Allard, B., Ittner, T., Torstenfelt, B: Migration of Trace Elements Into Water-Exposed Natural Fissure Surfaces of Granitic Rock, Chem. Geol. 49 (1985) 31-42.

Andersson, K., Torstenfelt, B., Allard, B: Diffusion of Cesium in Concrete, in J.G. Moore (Ed.), Scientific Basis for Nuclear Waste Management, Vol. 3, Plenum Press, New York 1981, pp. 235-242.

Birgersson, L., Neretnieks, I.: Diffusion in the matrix of granitic rock. Field test in the stripa mine. Part 2. SKBF/KBS TR 83-39, Stockholm 1983.

Crank, J: The Mathematics of Diffusion, 2nd Ed., Oxford University Press, London 1975.

Hultberg, B., Larson, S.-A., Tullborg, E.-L: Grundvatten i kristallin berggrund, Swedish Geol. Survey, SGU Dnr. 41.41.-81-4206-4, Uppsala 1981, (in Swedish).

Ittner, T., Torstenfelt, B., Allard, B.: Migration of neptunium, plutonium and americium in granitic rock. Radiocimica Acta, in press (1988a).

Ittner, T., Torstenfelt, B., Allard, B.: Migration of strontium, technetium, iodine and cesium in granitic rock. Radiocimica Acta, submitted (1988b).

Landström, O., Klockars, C.E., Persson, O., Andersson, K., Torstenfelt, B., Allard, B., Larson, S.-A., Tullborg, E.-L: A Comparison of In-Situ Radionuclide Migration Studies in the Studsvik Area and Laboratory Measurements, in W. Lutze (Ed.), Scientific Basis for Nuclear Waste Management - V, Elsevier, New York 1982, pp. 698-706.

Laurent, S: Analysis of Groundwater From Deep Boreholes in Kråkemåla, Sternö and Finnsjön, SKBF/KBS TR 82-23, SKB, Stockholm 1982.

Nordstrom, D.K., Andrews, J.N., Carlsson, L., Fontes, J.-C., Fritz, P., Moser, H., Olsson, T: Hydrogeological and hydrogeochemical investigations in boreholes - Final report of the phase I geochemical investigations of the Stripa groundwaters. Stripa project 85-06, SKB, Stockholm 1985.

Skagius, K., Neretnieks, I.: Diffusivity measurements and electrical resistivity measurements in rock samples under mechanical stress. SKB TR 85-05, Stockholm 1985.

Torstenfelt, B: Migration of the Fission Products Strontium, Technetium, Iodine and Cesium in Clay, *Radiochim. Acta* 39, 97-104 (1986a).

Torstenfelt, B: Migration of the Actinides Thorium, Protactinium, Uranium, Neptunium, Plutonium and Americium in Clay, *ibid*, 105-112 (1986b).

Torstenfelt, B., Ittner, T., Allard, B., Andersson, K., Olofsson, U: Mobilities of Radionuclides in Fresh and Fractured Crystalline Rock, SKBF/KBS TR 82-26, SKB, Stockholm 1982a.

Torstenfelt, B., Andersson, K., Allard, B: Sorption of Strontium and Cesium on Rocks and Minerals, *Chem. Geol.* 36 (1982b) 123-137.

Tullborg, E.-L., Larson, S.-A: Fissure Fillings From Finnsjön and Studsvik, Sweden, Identification, Chemistry and Dating, SKBF/KBS TR 82-20, SKB, Stockholm 1982.

Wollenberg, H., Flexser, S., Andersson, L: Petrology and radiogeology of the stripa pluton, LBL-11654, 1982.

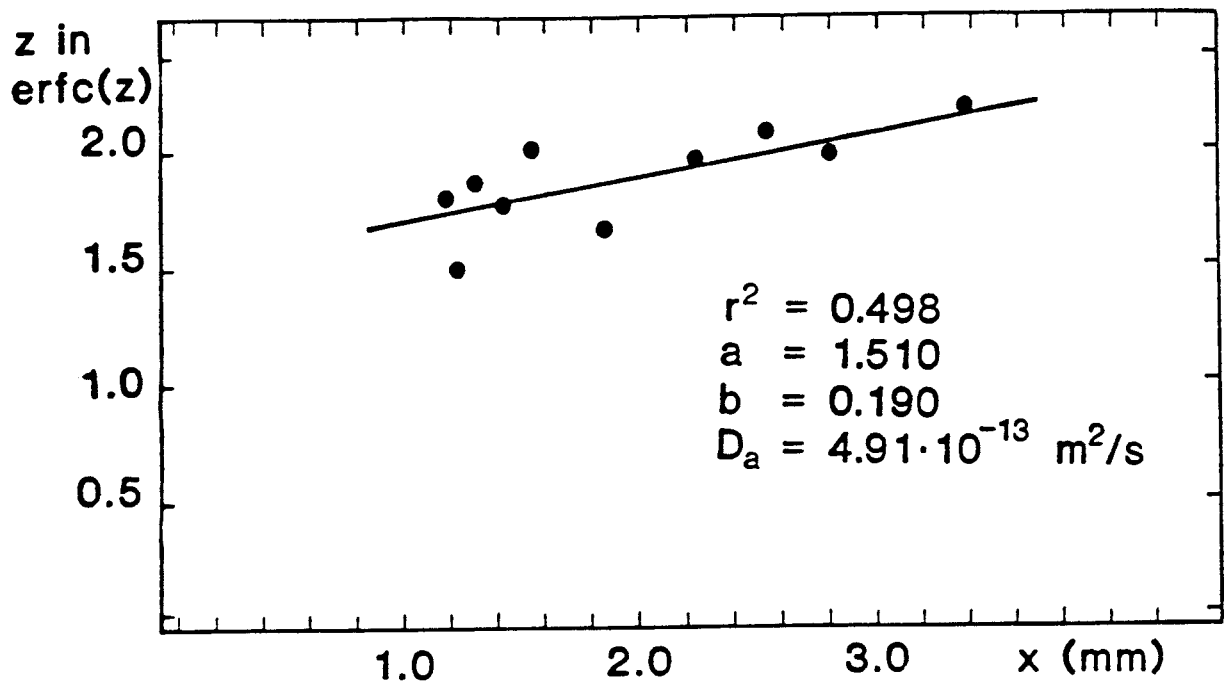


Fig 1 Diffusion of strontium in Finnsjö granite(Fi7 526.5)
 Diffusion time 164 days. cf., Fig 38.

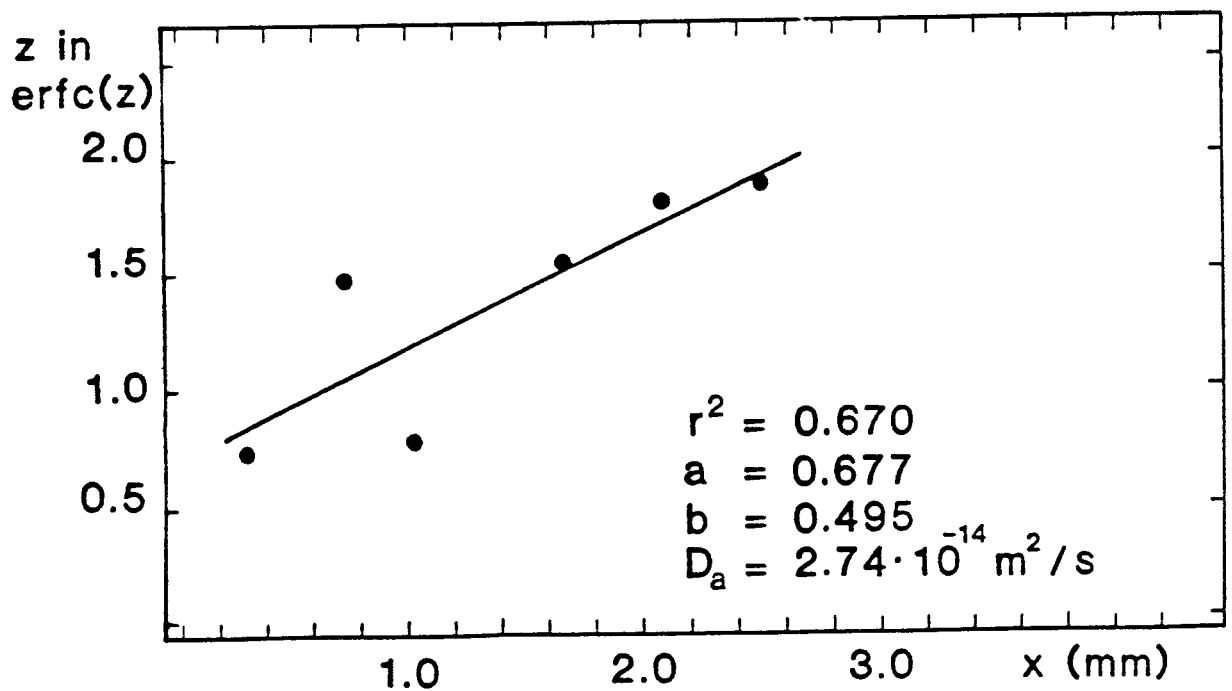


Fig 2. Diffusion of strontium in Stripa granite(Str 2:2)
 Diffusion time 432 days. cf., Fig 39.

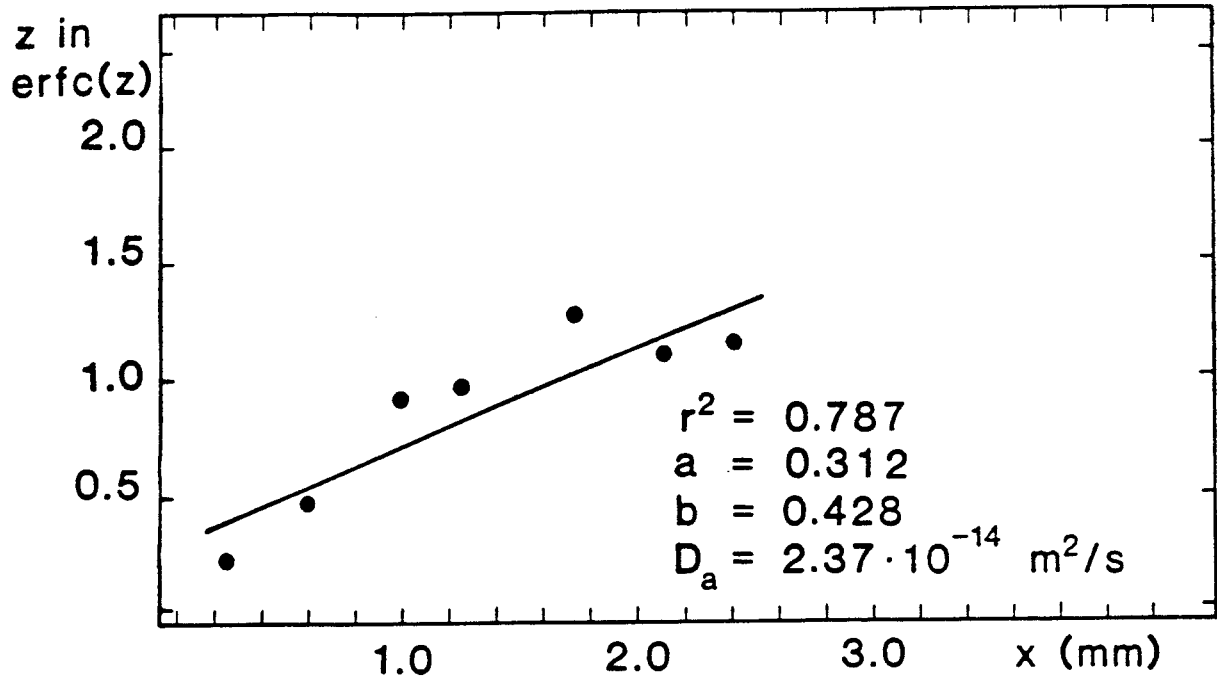


Fig 3. Diffusion of strontium in Studsvik gneiss(Stu 6:3)
 Diffusion time 657 days. cf., Fig 40.

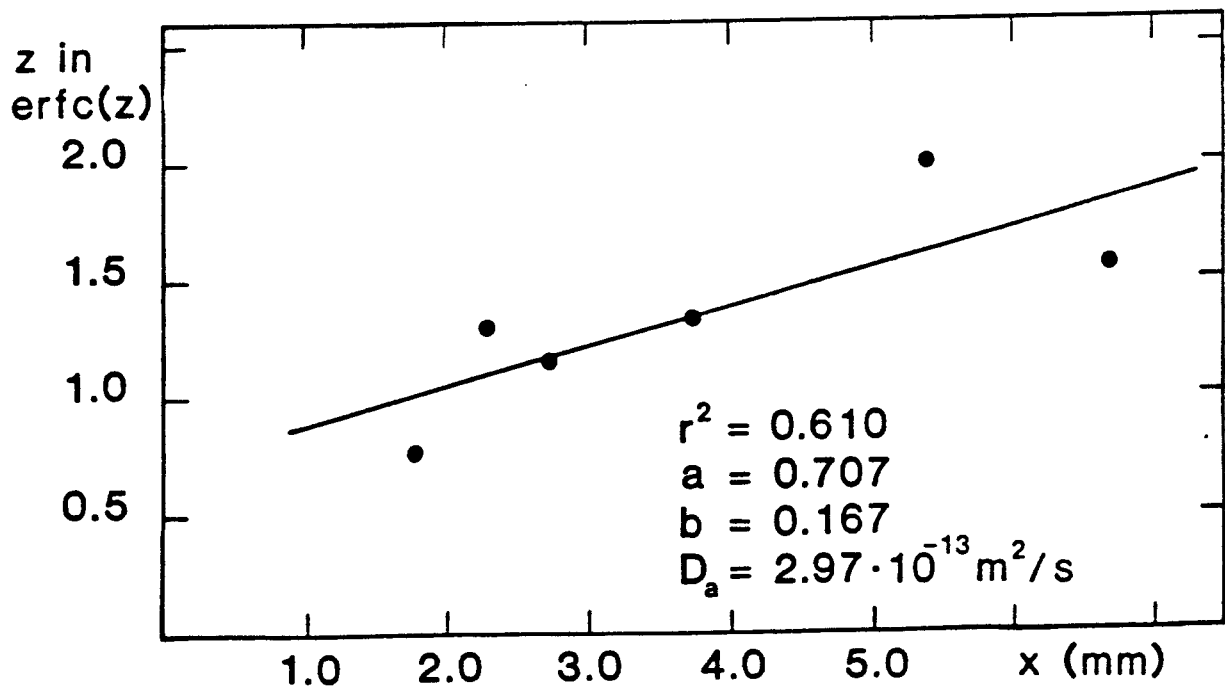


Fig 4. Diffusion of technetium in Finnsjö granite(Fi6 309.0:4)
 (calcite). Diffusion time 349 days.

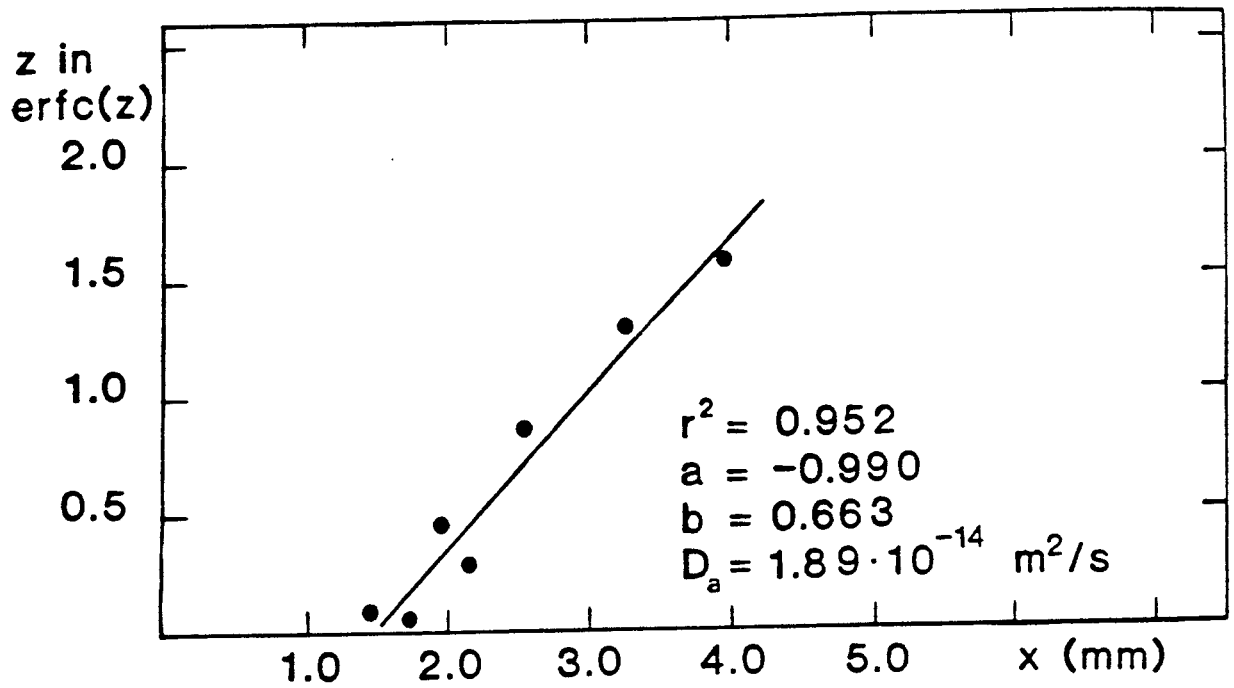


Fig 5. Diffusion of technetium in Finnsjö granite(Fi7 318.8:4)
Diffusion time 349 days.

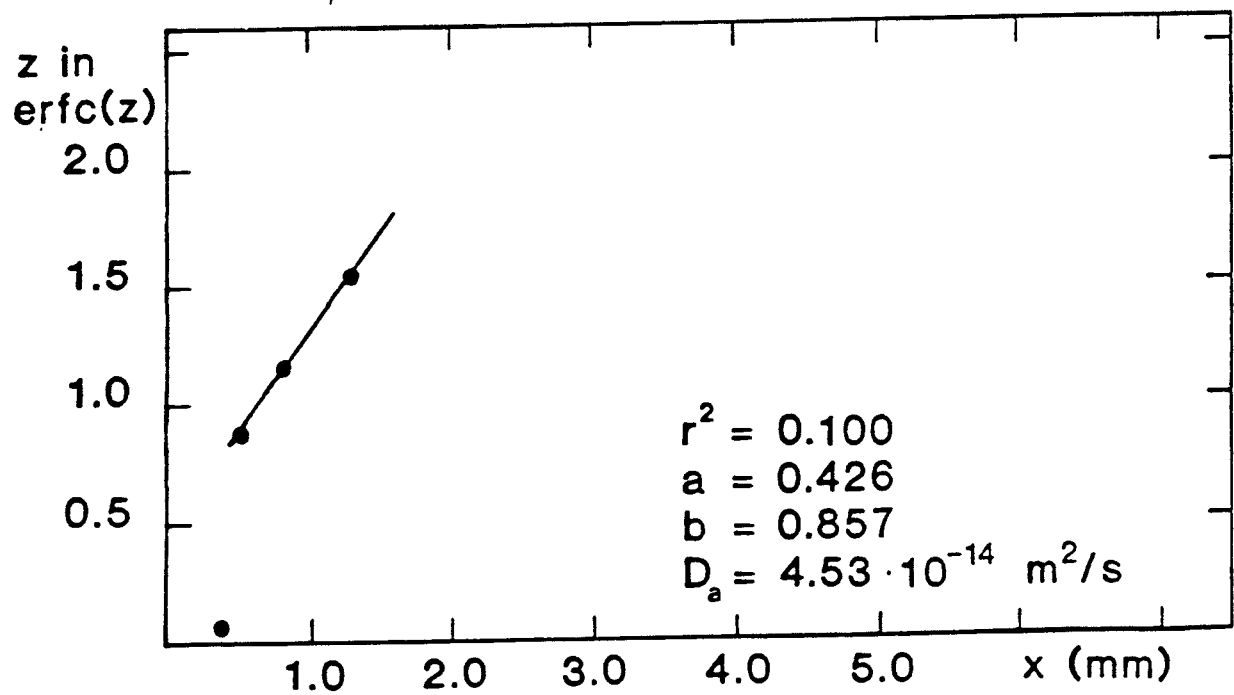


Fig 6. Diffusion of technetium in Finnsjö granite(Fi7 526.5:4r)
Diffusion time 87 days.

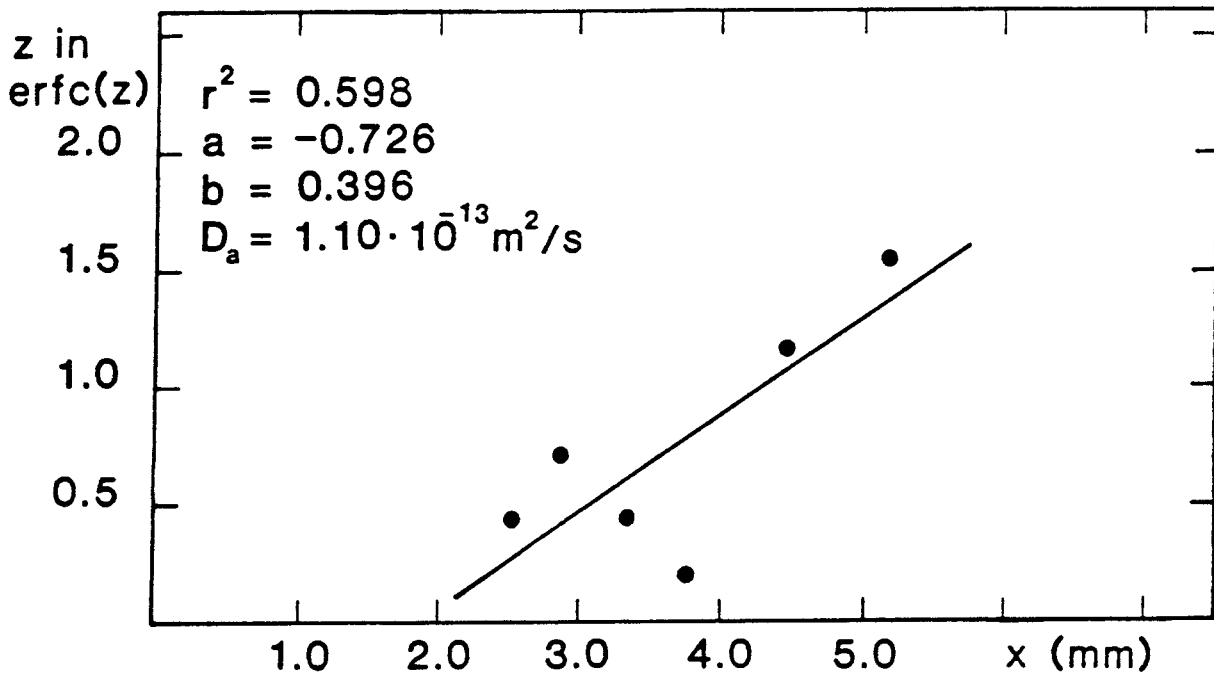


Fig 7. Diffusion of technetium in Finnsjö granite(Fi8 72.0:3)
 Diffusion time 167 days.

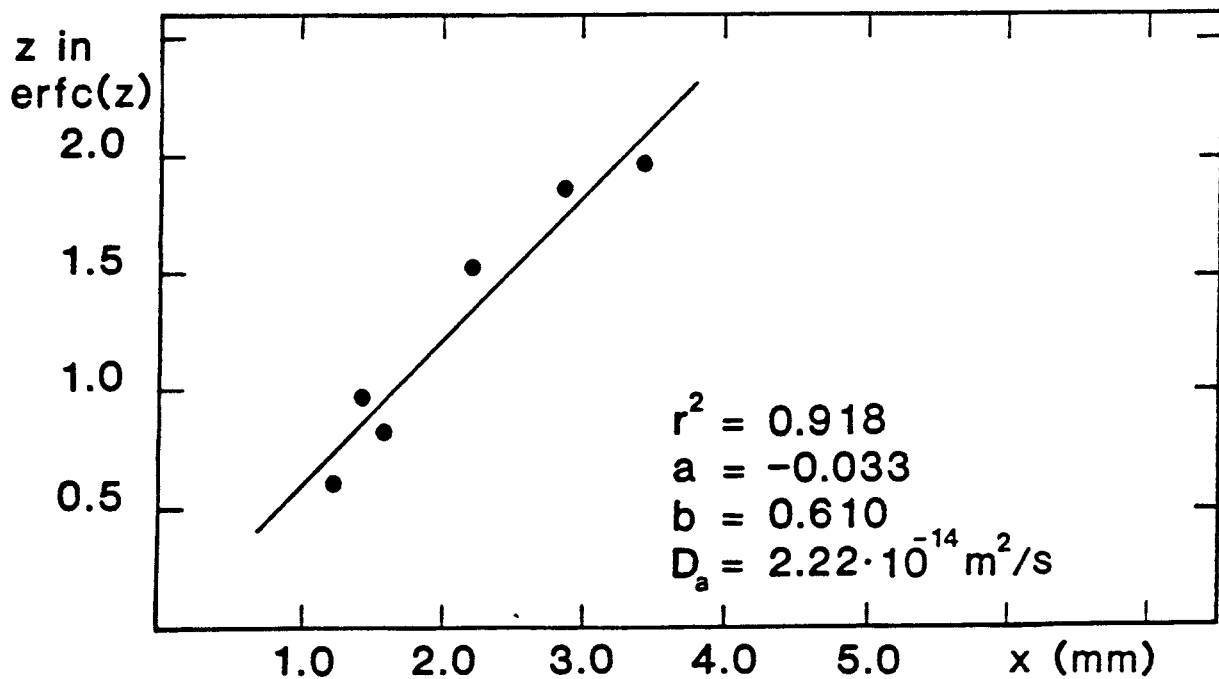


Fig 8. Diffusion of technetium in Finnsjö granite(Fi8 134.8:3)
 Diffusion time 349 days.

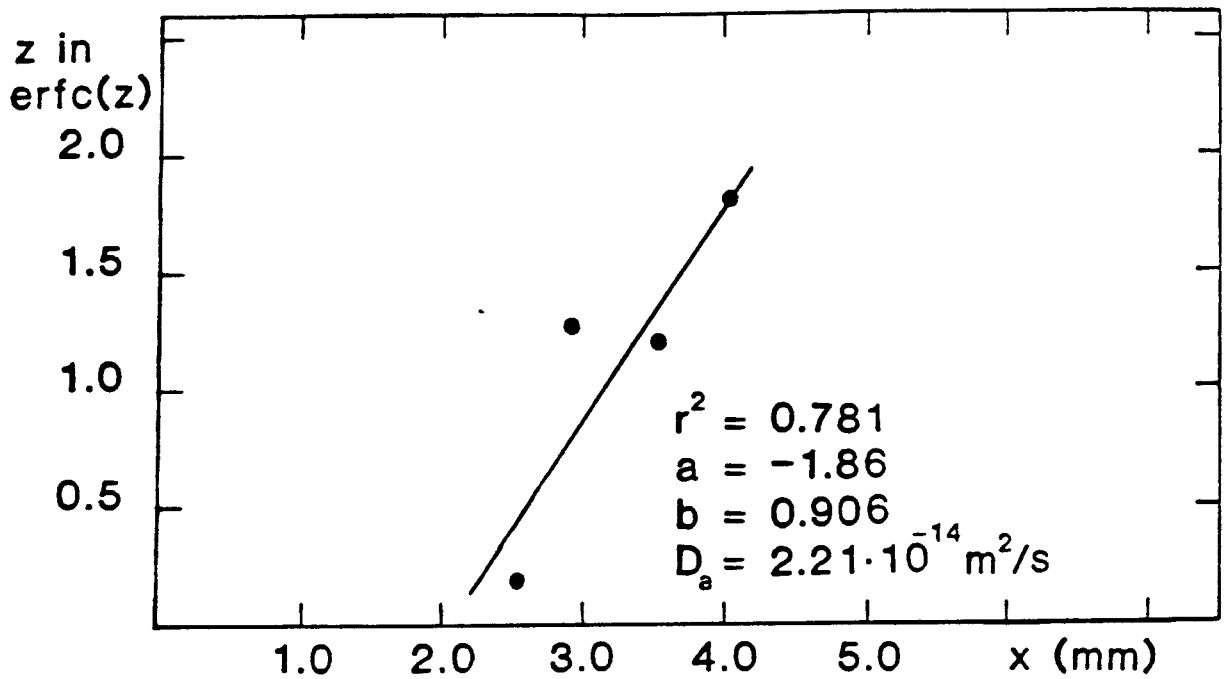


Fig 9. Diffusion of technetium in Studsvik gneiss(Stu 29.3:3)
 Diffusion time 167 days.

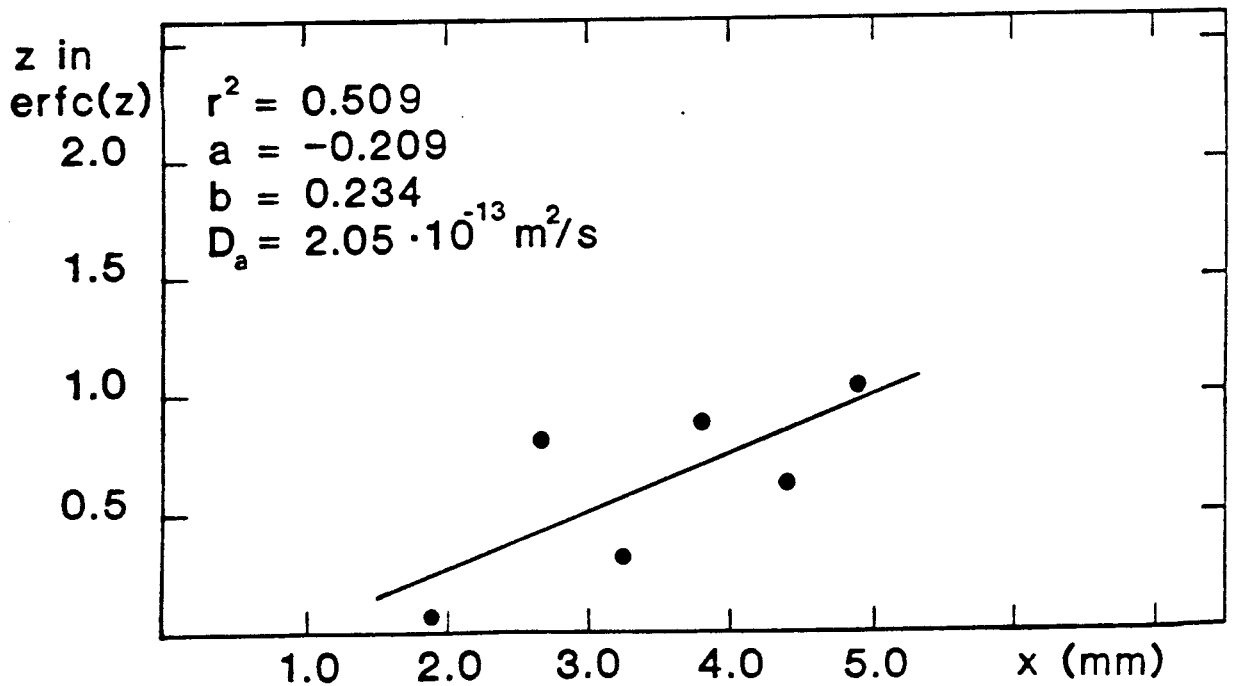


Fig 10. Diffusion of technetium in Stripa granite(Str A:3N)
 Diffusion time 257 days.

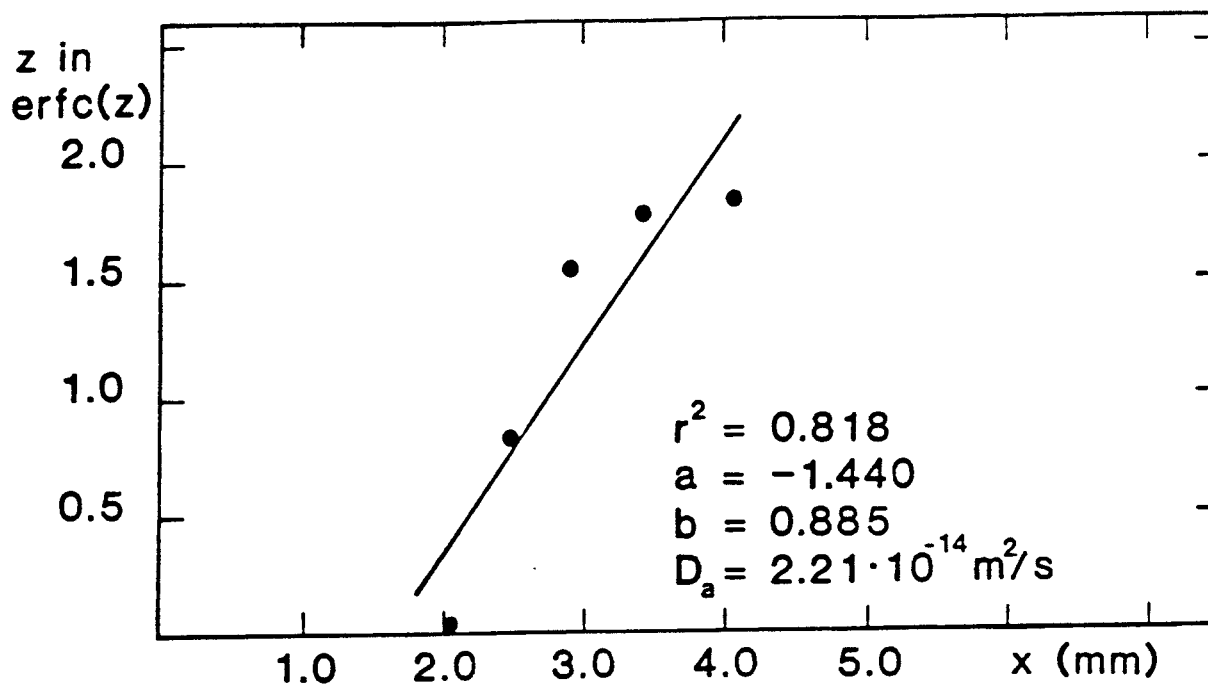


Fig 11. Diffusion of technetium in Stripa granite(Str 1:5)
Diffusion time 167 days.

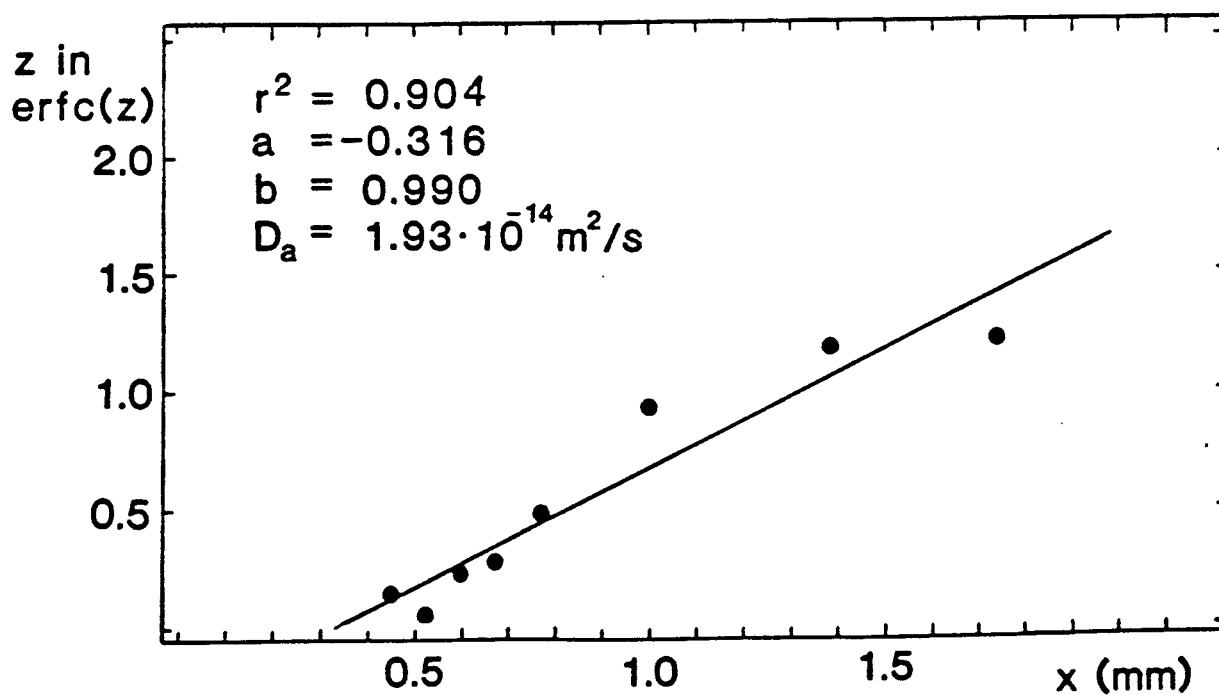


Fig 12. Diffusion of iodine in Finnsjö granite(Fi B:2)
Diffusion time 153 days.

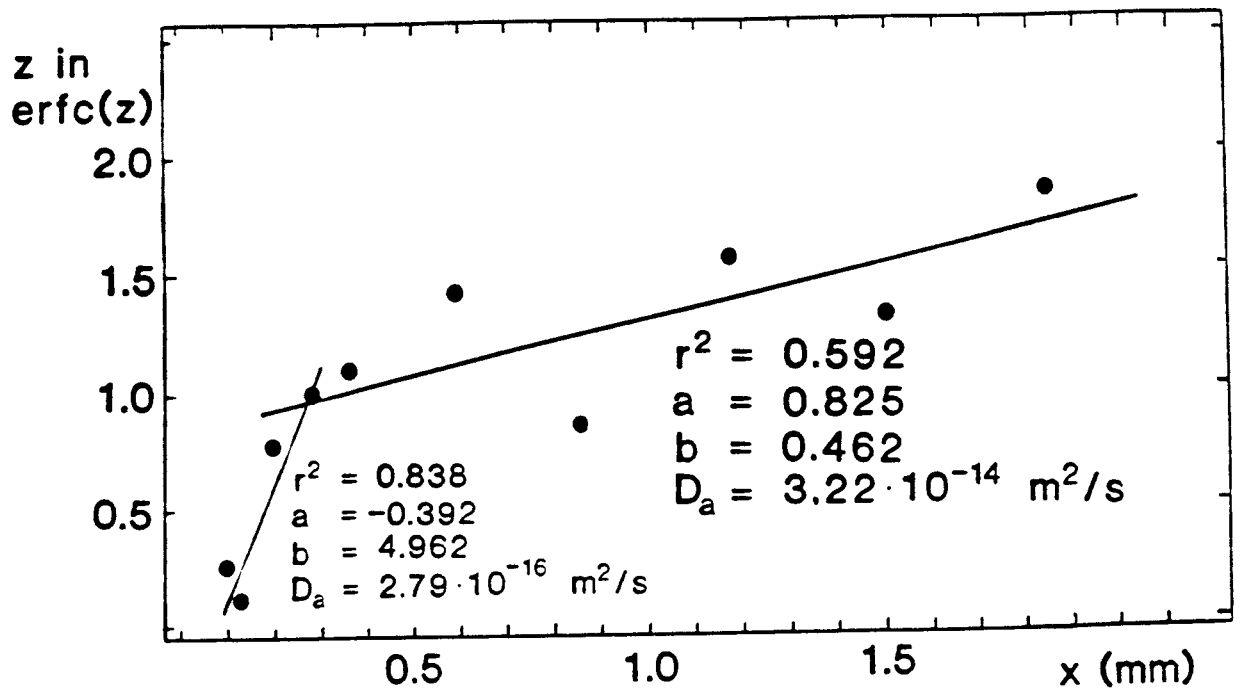


Fig 13. Diffusion of iodine in Stripa granite(Str 2:1)
 Diffusion time 421 days. cf., Fig 41.

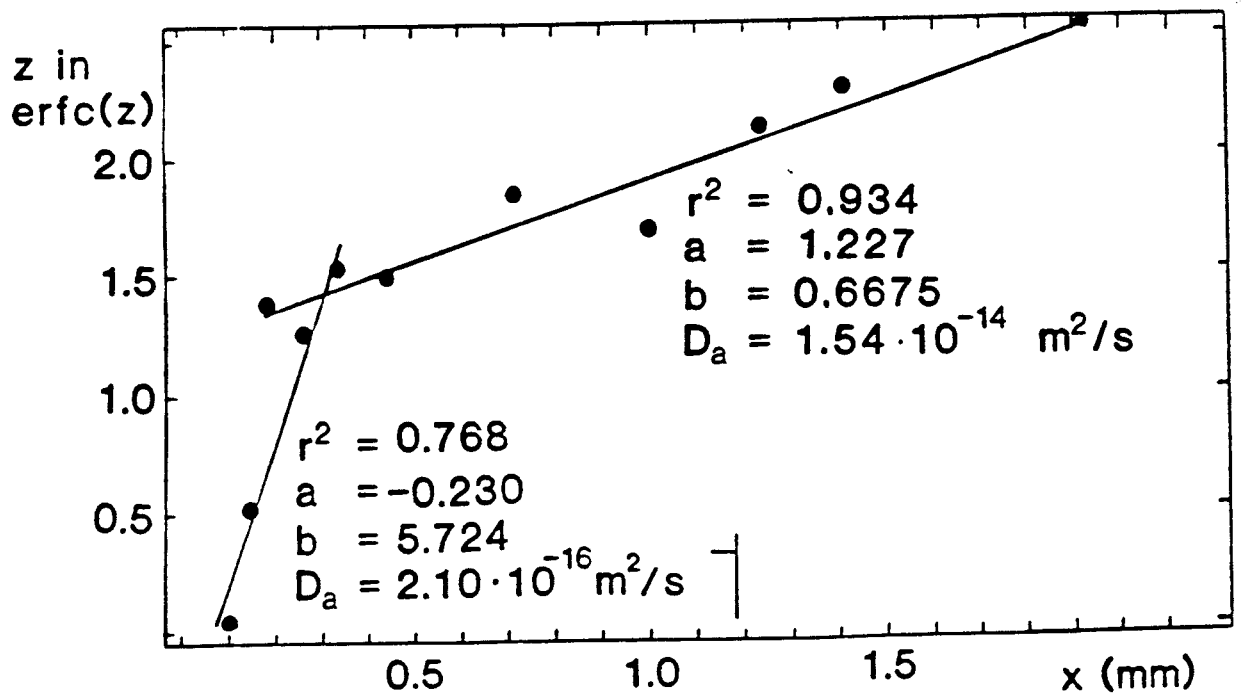


Fig 14. Diffusion of iodine in Studsvik gneiss(Stu A:2)
 Diffusion time 421 days. cf., Fig 42.

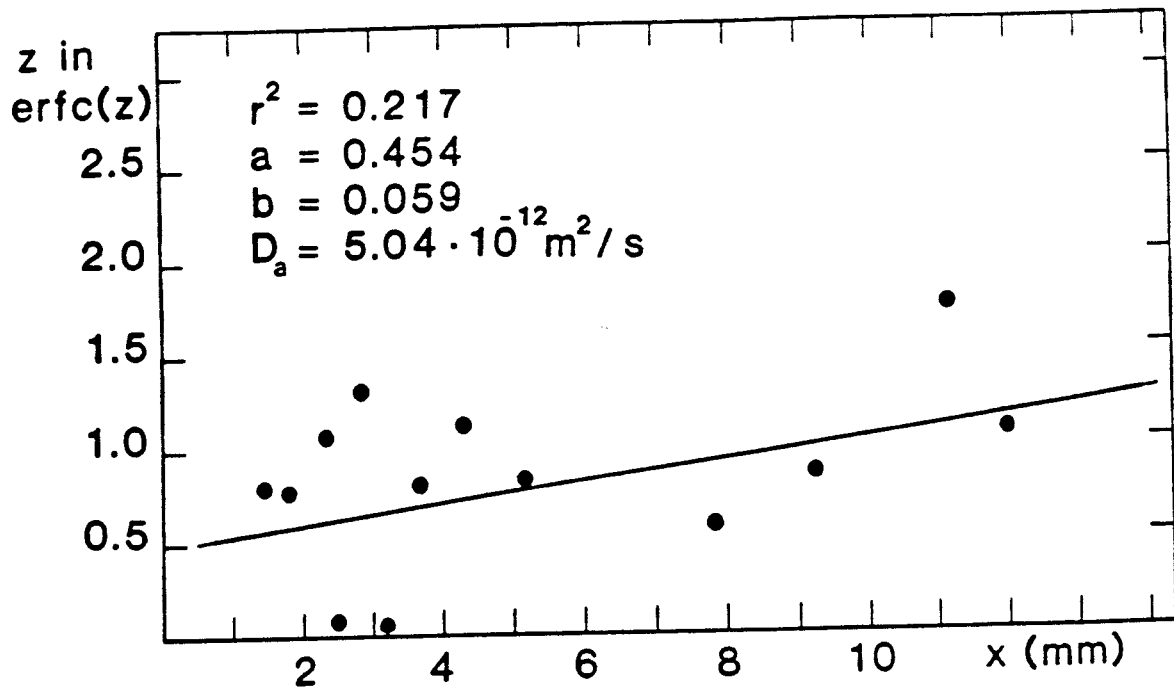


Fig 15. Diffusion of cesium in Finnsjö granite(Fi6 309.0:1) (calcite). Diffusion time 167 days. cf., Fig 43.

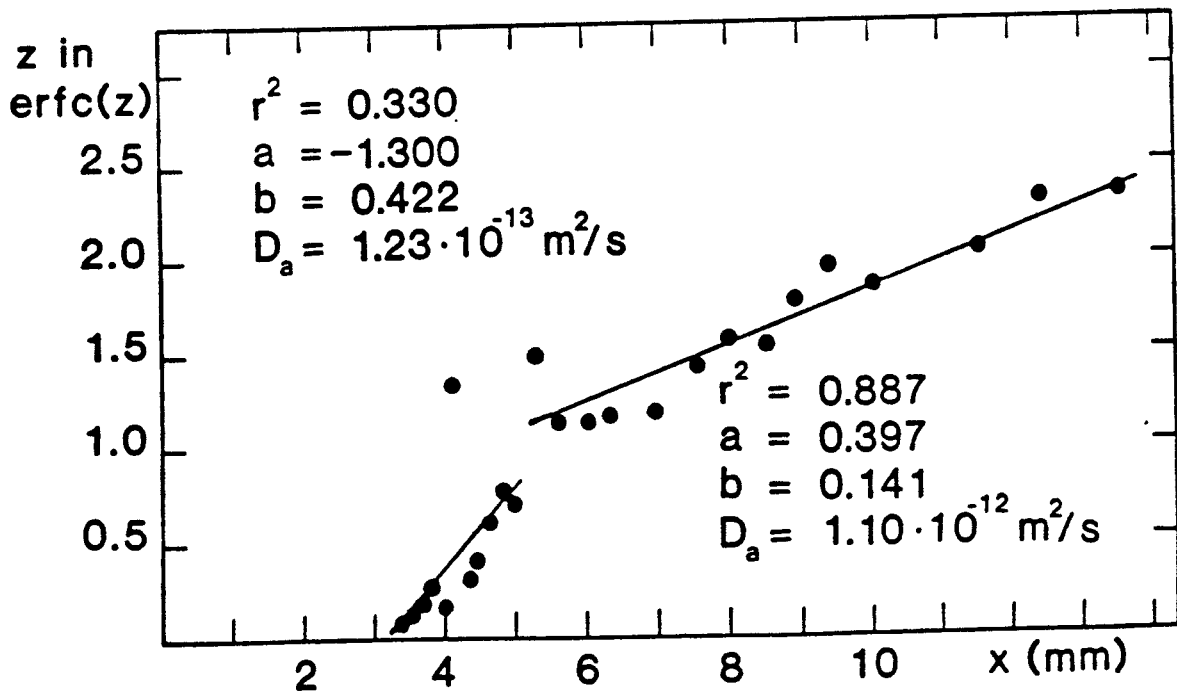


Fig 16. Diffusion of cesium in Finnsjö granite(Fi7 318.8:1) Diffusion time 132 days. cf., Fig 44.

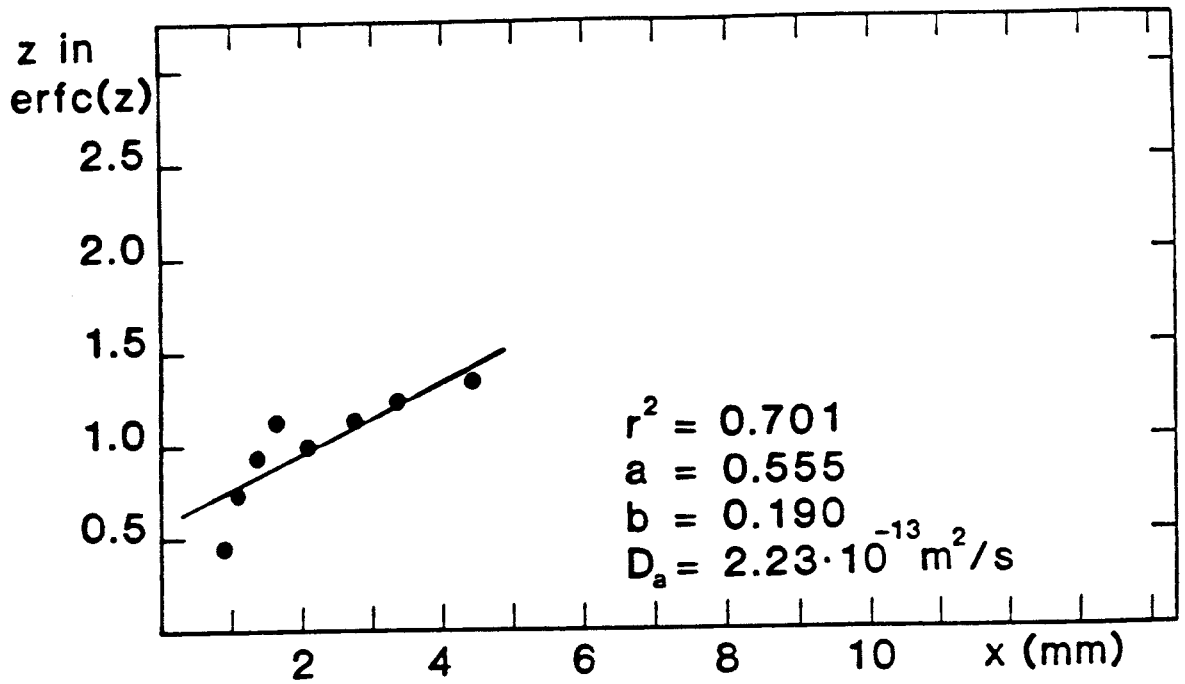


Fig 17. Diffusion of cesium in Finnsjö granite(Fi7 526.5:2r)
Diffusion time 357 days.

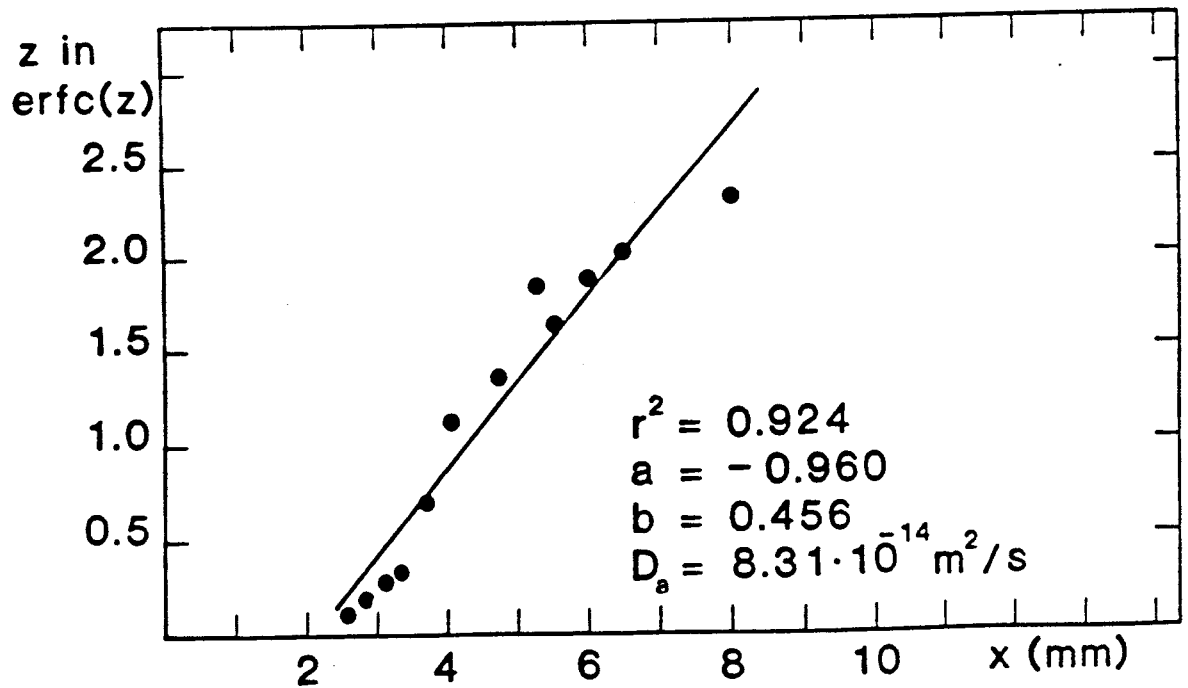


Fig 18. Diffusion of cesium in Finnsjö granite(Fi8 72.0:1)
Diffusion time 167 days.

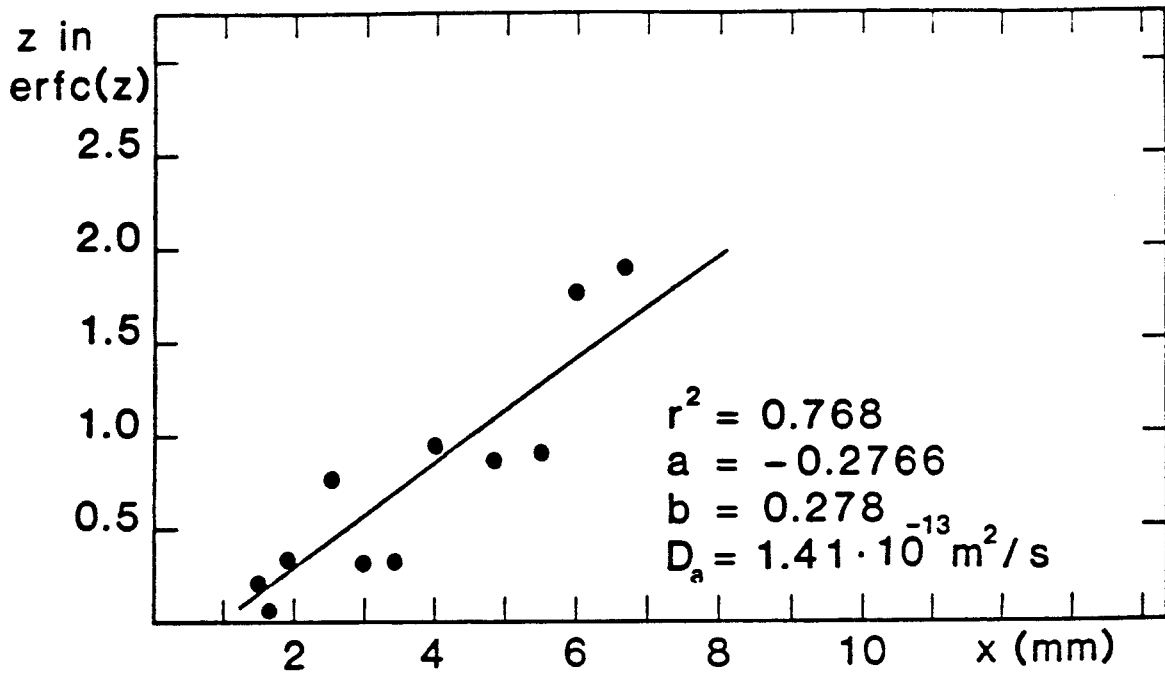


Fig 19. Diffusion of cesium in Finnsjö granite(Fi8 358.1:1)
 Diffusion time 265 days.

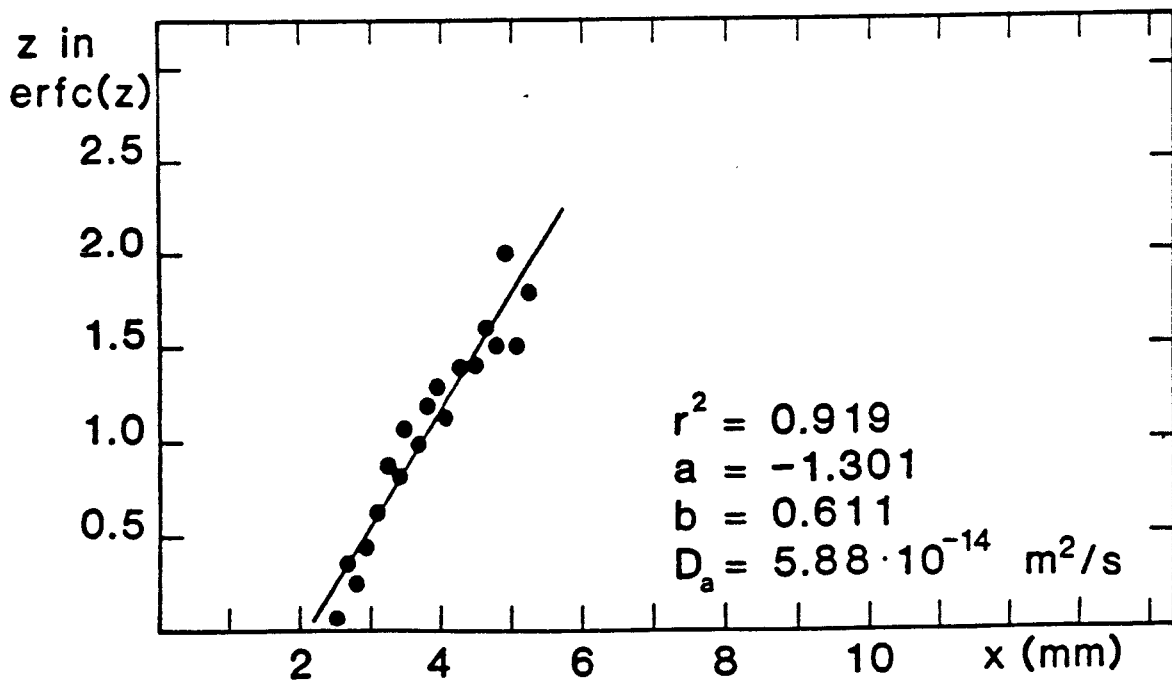


Fig 20. Diffusion of cesium in Studsvik gneiss(Stu 5.4:1)
 Diffusion time 132 days. cf., Fig 45.

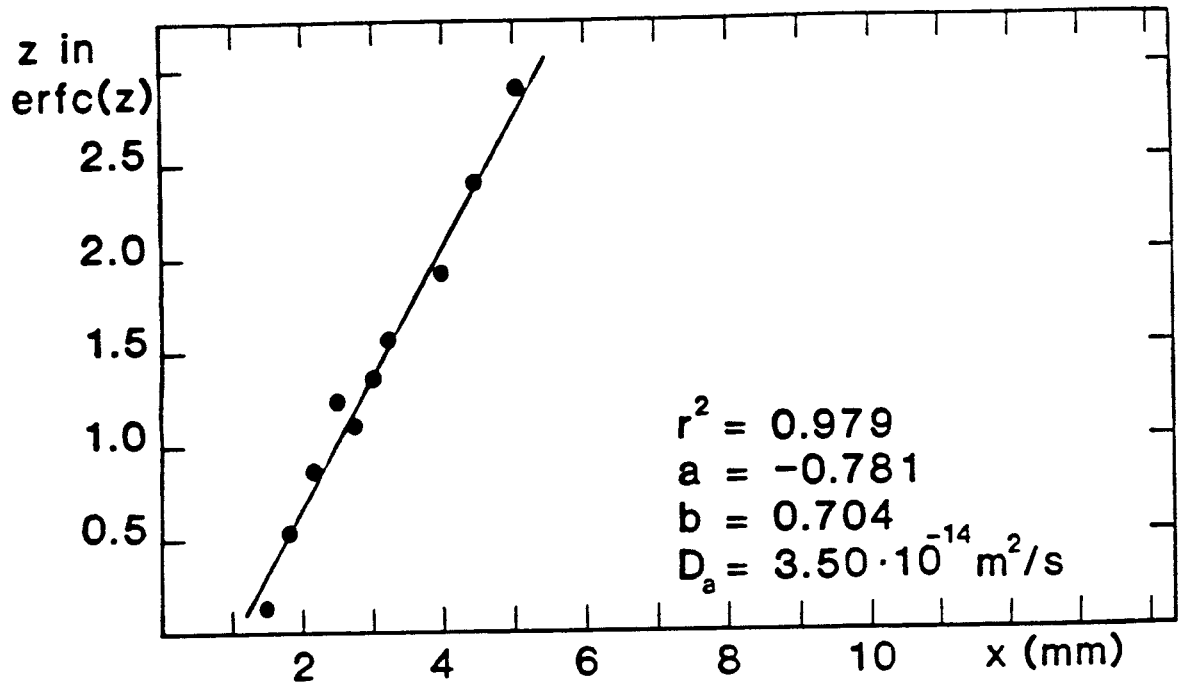


Fig 21. Diffusion of cesium in Studsvik gneiss(Stu 104.2)
 Diffusion time 167 days.

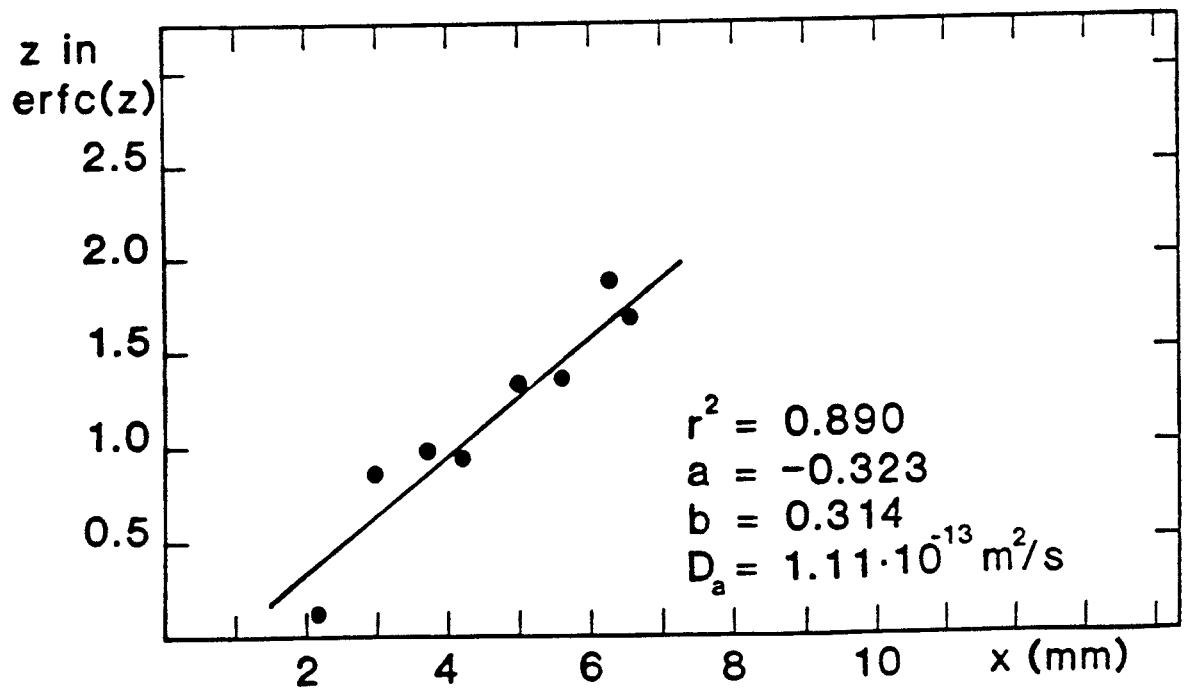


Fig 22. Diffusion of cesium in Studsvik gneiss(Stu 183.1:1)
 Diffusion time 265 days.

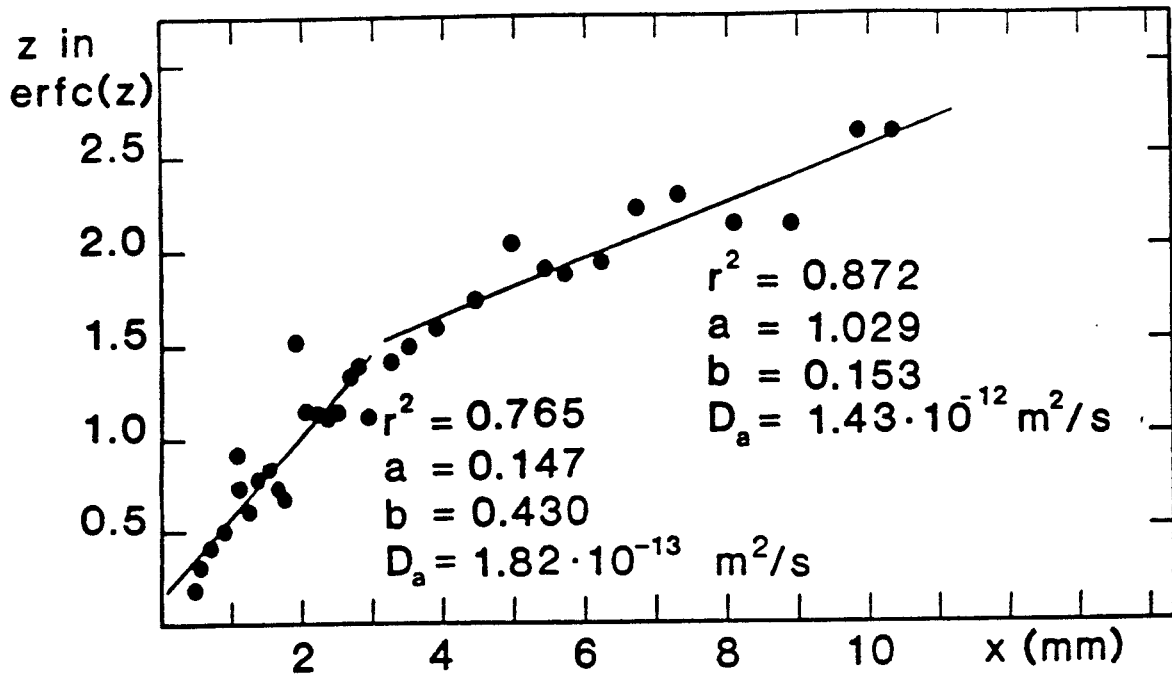


Fig 23. Diffusion of cesium in Stripa granite(Str A:1vr)
Diffusion time 85 days.

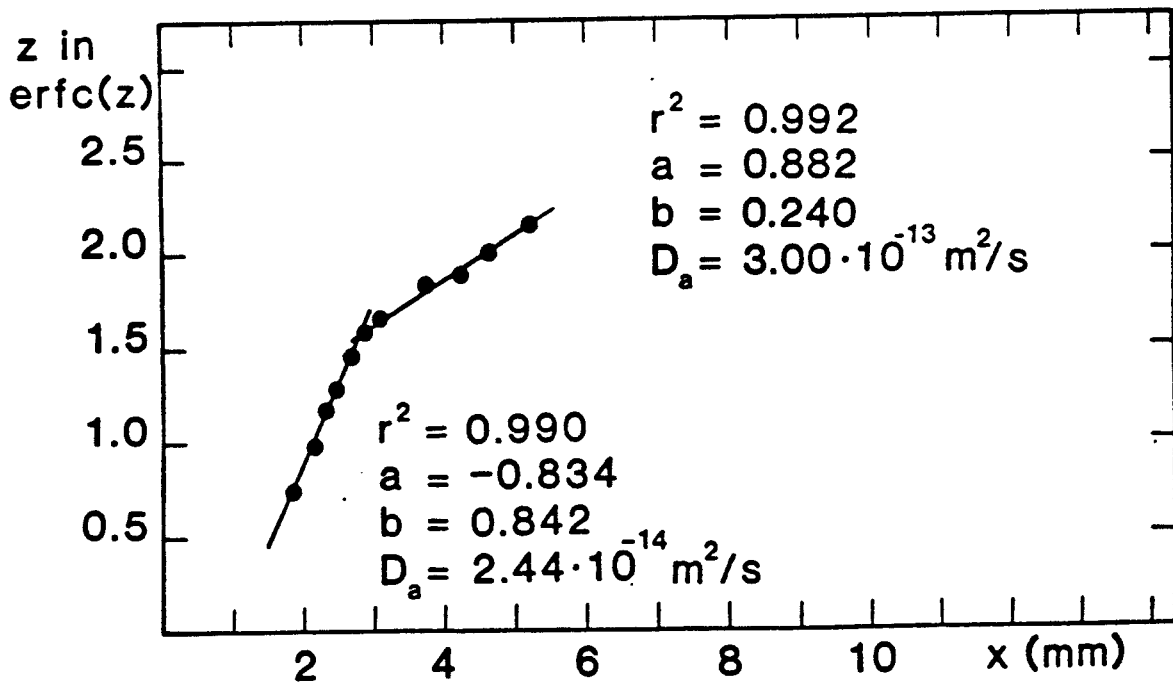


Fig 24. Diffusion of cesium in Stripa granite(Str A:1N)
Diffusion time 167 days.

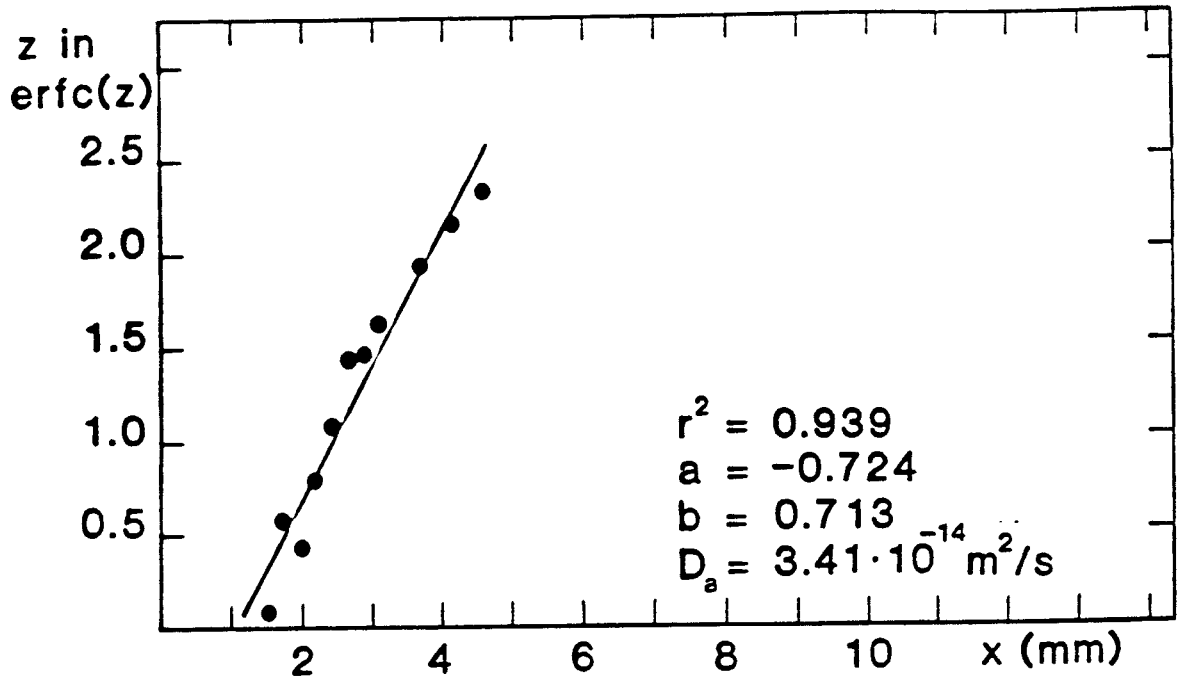


Fig 25. Diffusion of cesium in Stripa granite(Str MS:2)
 Diffusion time 167 days. cf., Fig 46.

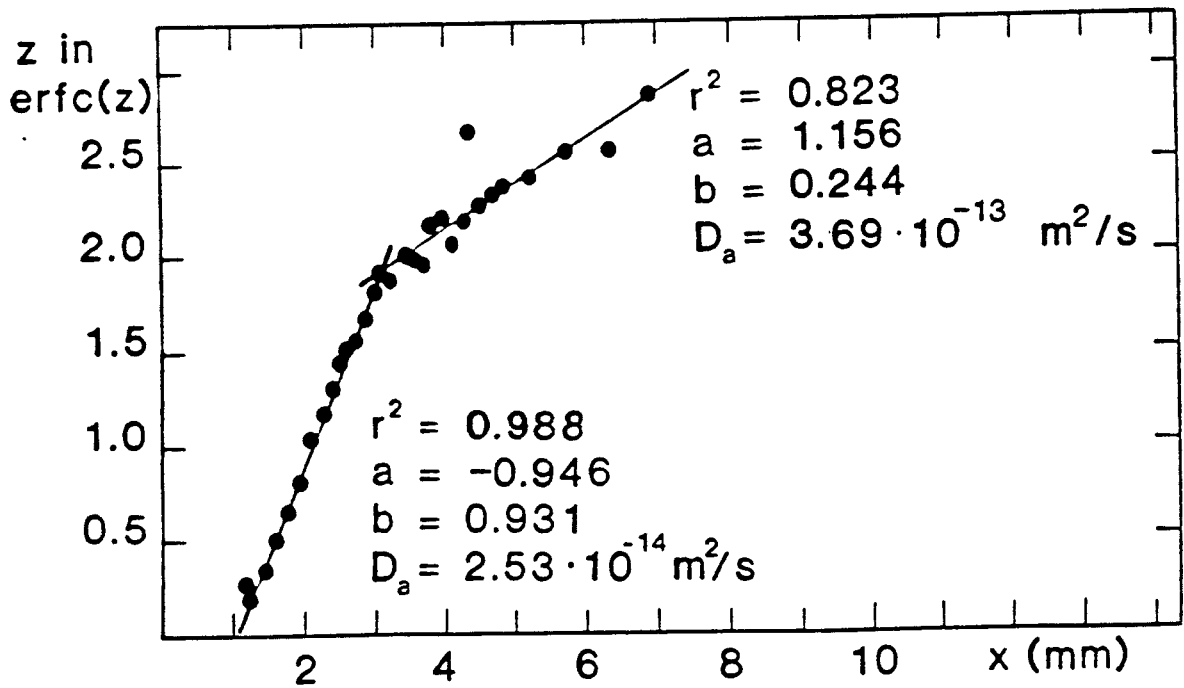


Fig 26. Diffusion of cesium in Stripa granite(Str 1:1)
 Diffusion time 132 days.

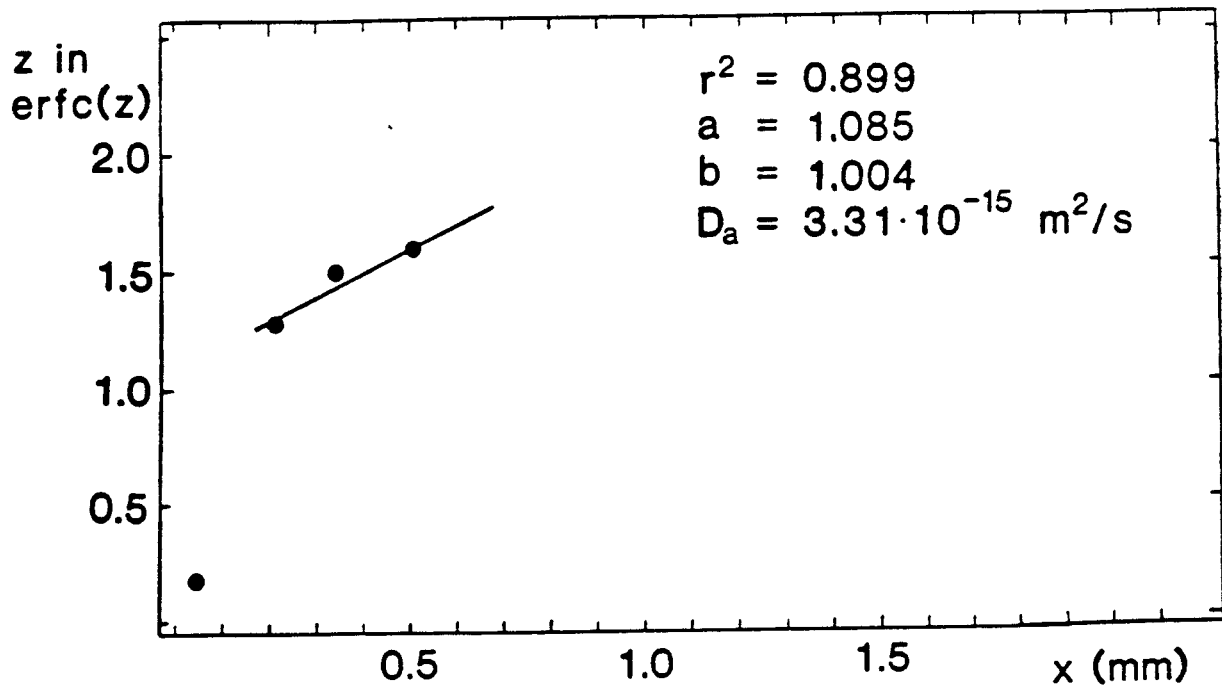


Fig 27. Diffusion of neptunium in Finnsjö granite(Fi8 358.1:1)
 Diffusion time 866 days. cf., Fig 47.

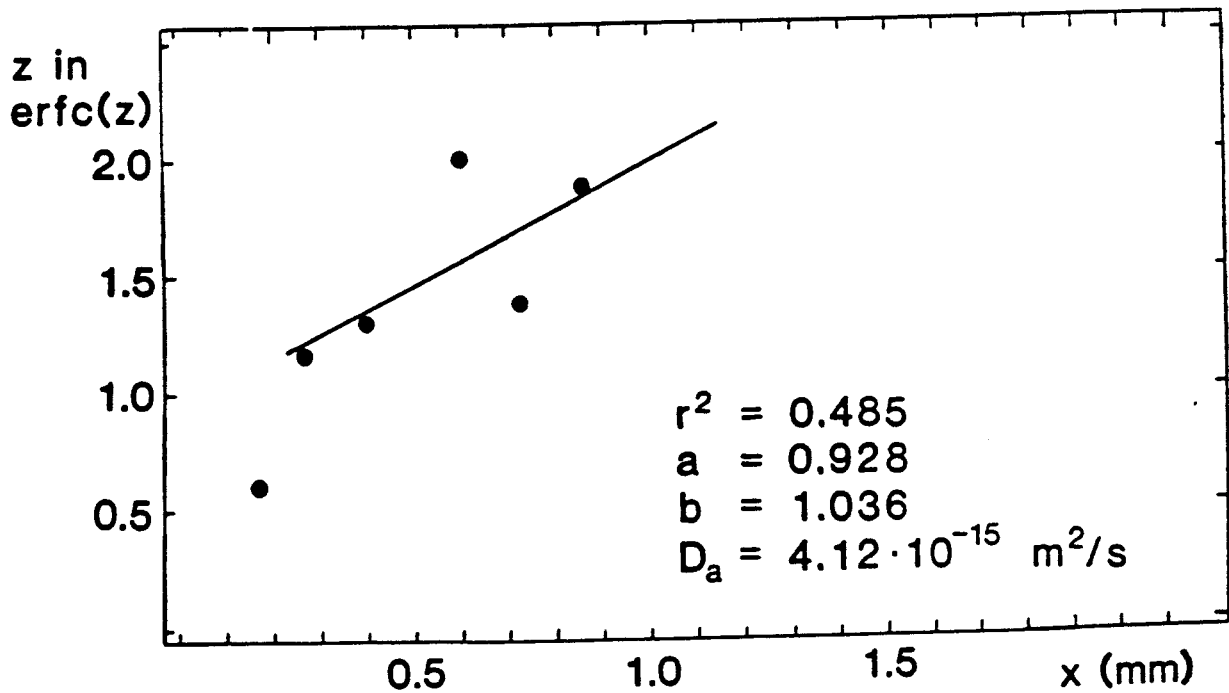


Fig 28. Diffusion of neptunium i Stripa granite(Str 3:4)
 Diffusion time 654 days. cf., Fig 48.

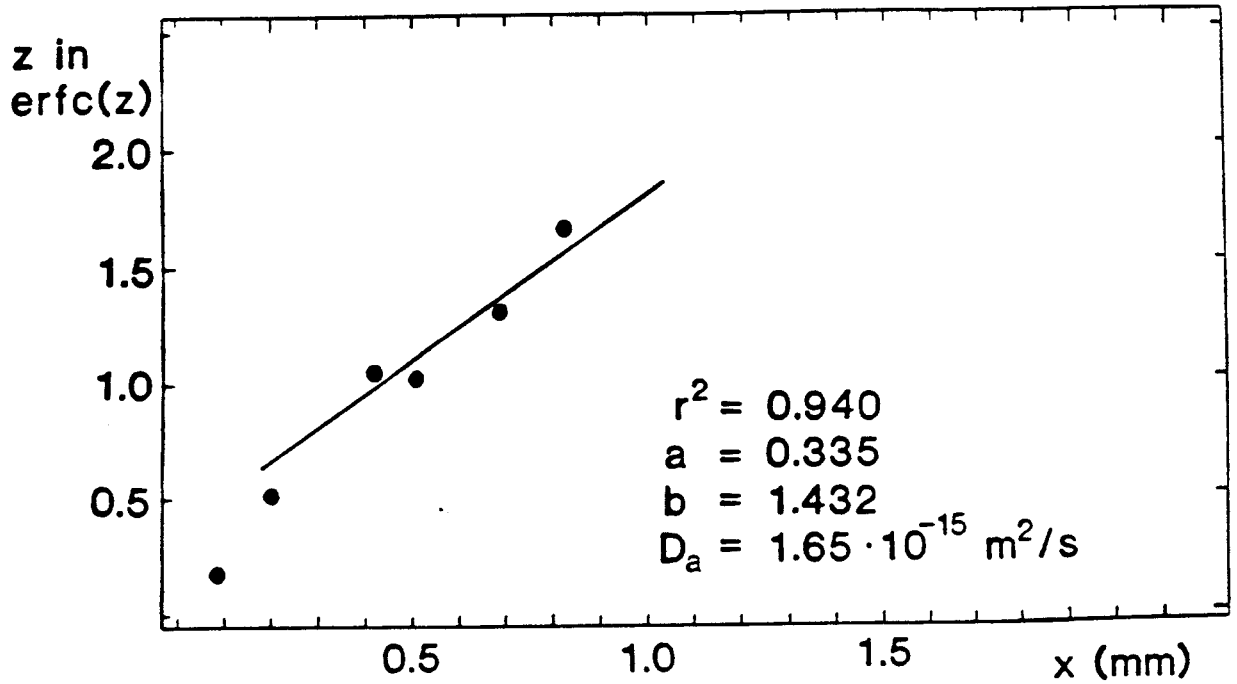


Fig 29. Diffusion of plutonium in Finnsjö granite(Fi8 358.1:2)
 Diffusion time 854 days. cf., Fig 49.

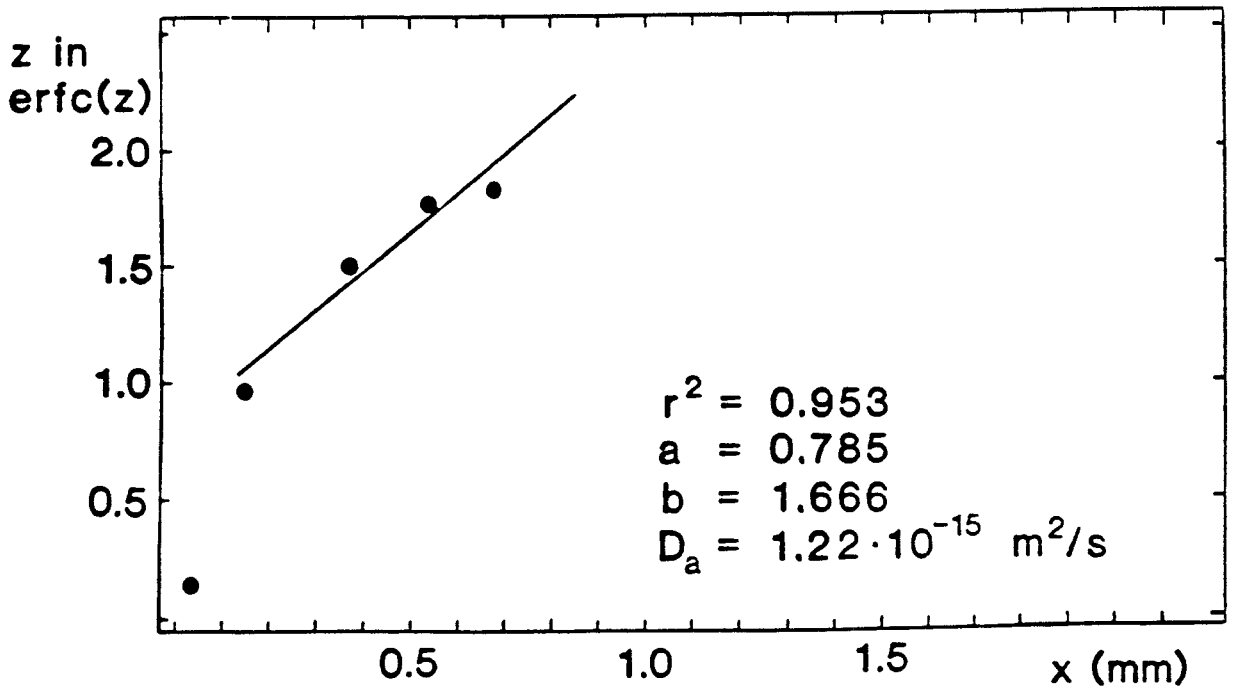


Fig 30. Diffusion of plutonium in Stripa granite(Str 4:2)
 Diffusion time 858 days. cf., Fig 50.

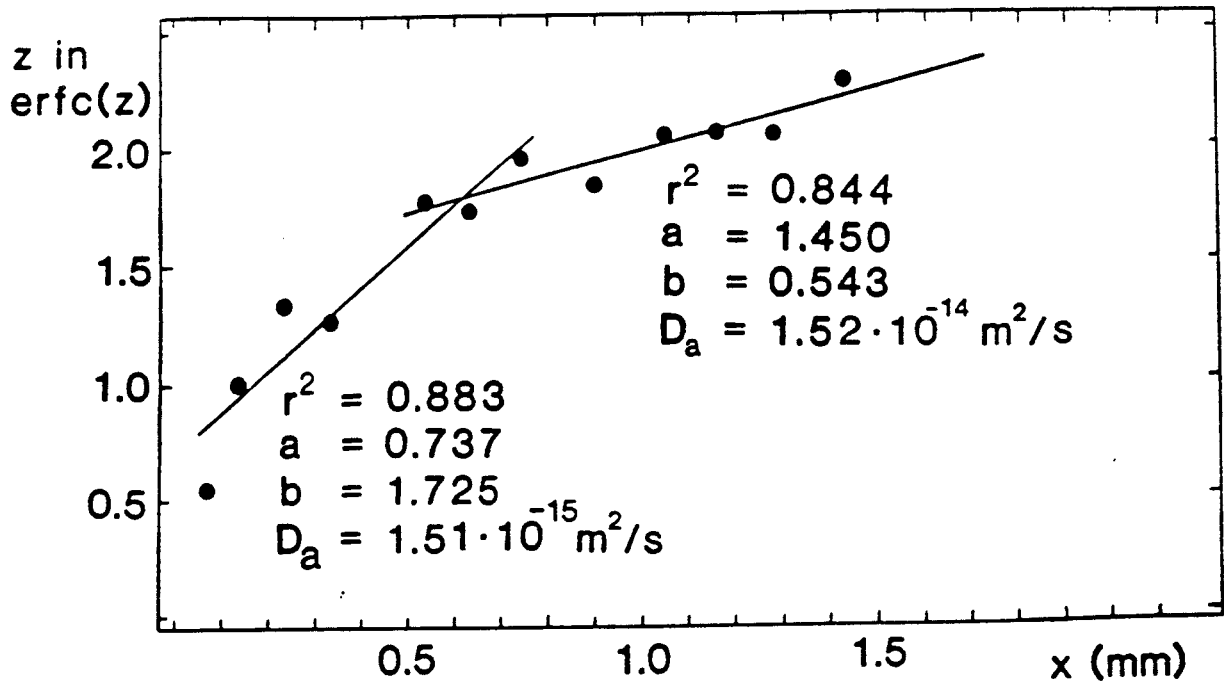


Fig 31. Diffusion of plutonium in Stripa granite(Str 4:1)
 Diffusion time 646 days. cf., Fig 51.

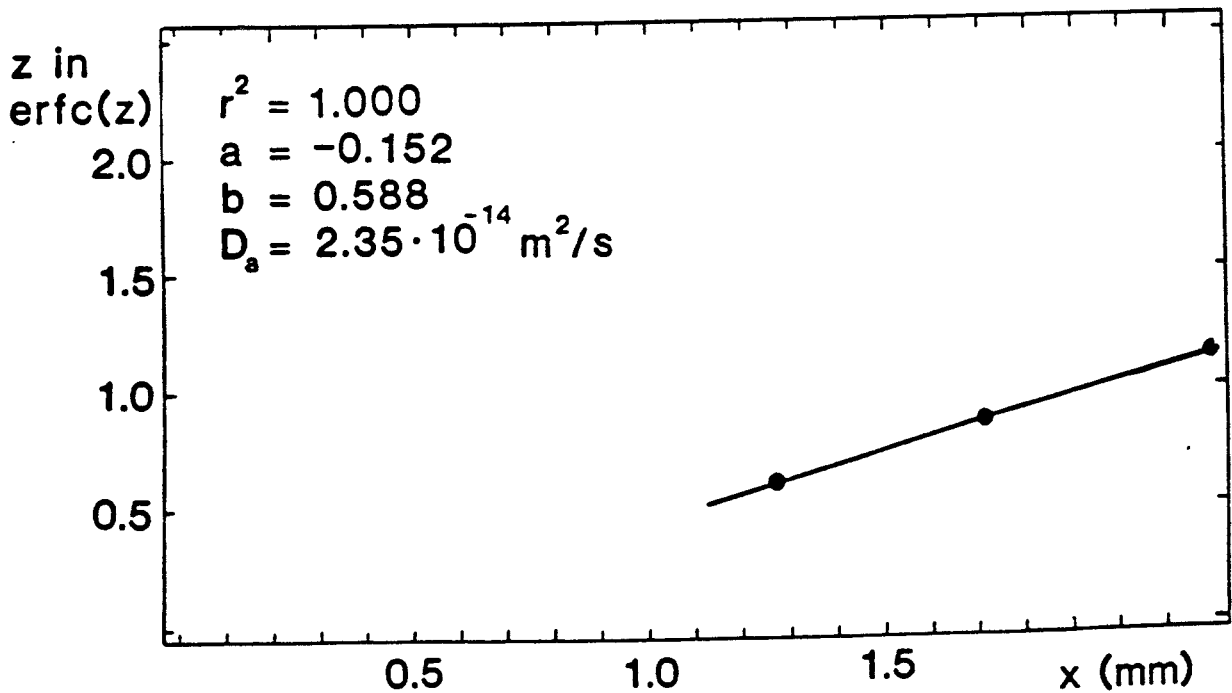


Fig 32. Diffusion of americium in Finnsjö granite(Fi6 309.0:3)
 (calcite). Diffusion time 355 days.

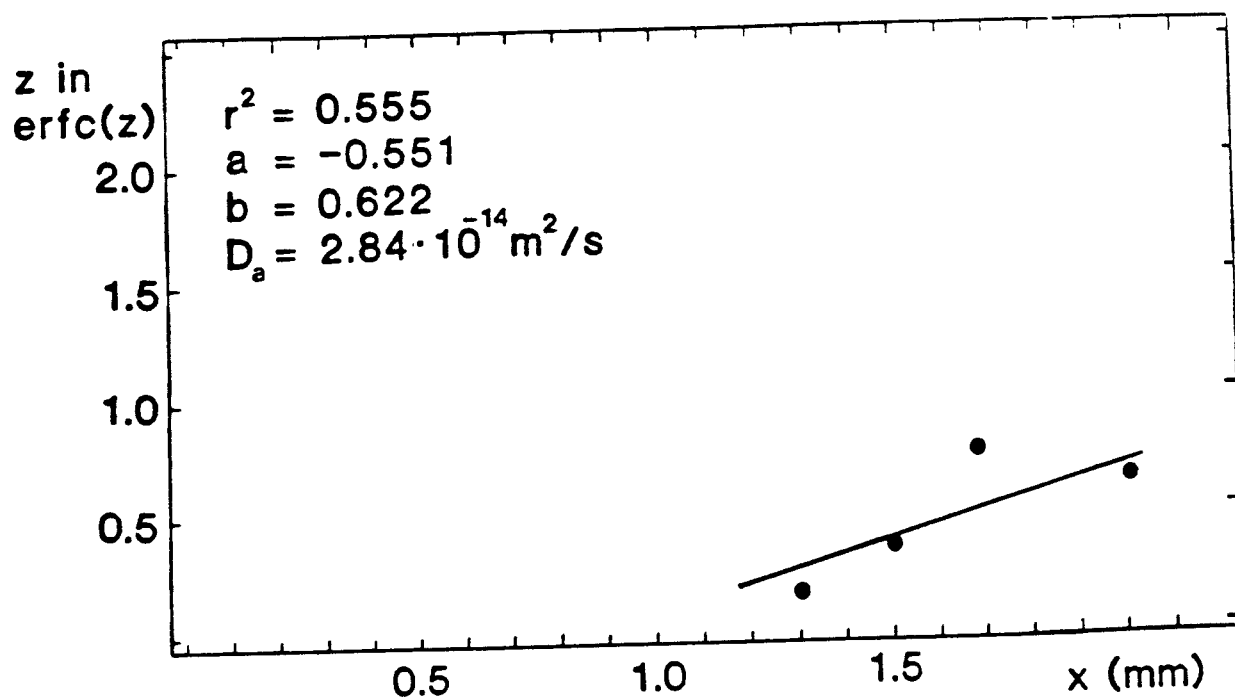


Fig 33. Diffusion of americium in Finnsjö granite(Fi7 526.5:3)
Diffusion time 263 days.

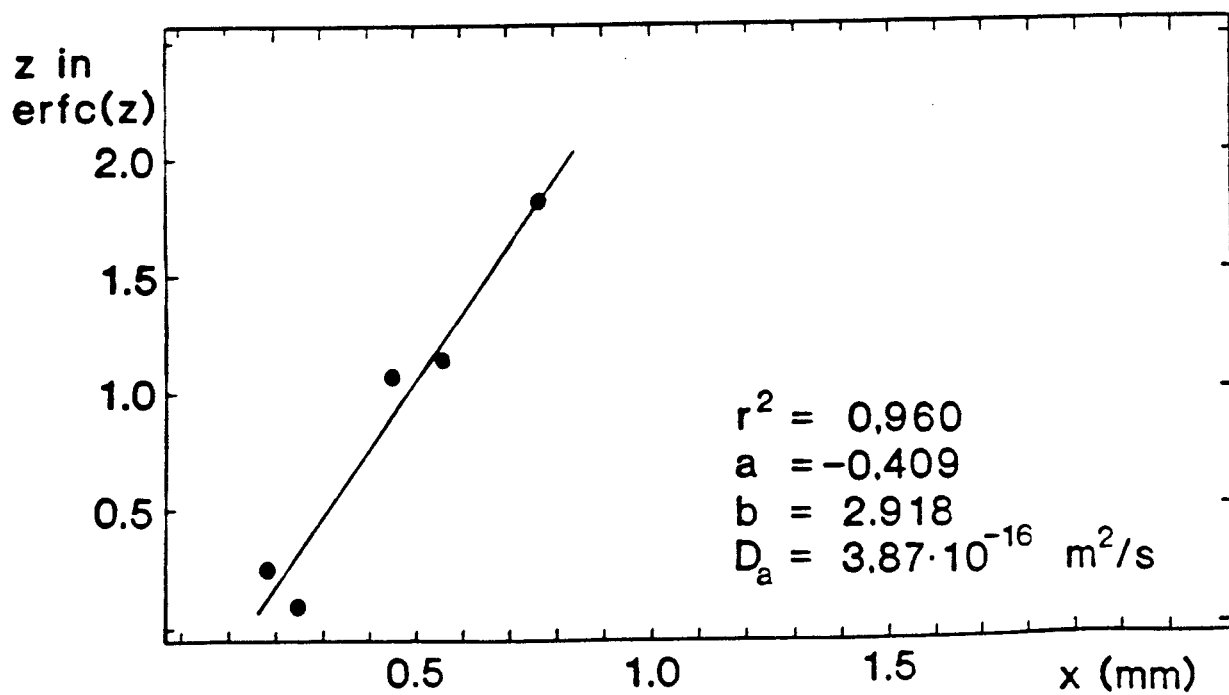


Fig 34. Diffusion of americium in Finnsjö granite(Fi8 358.1:3)
Diffusion time 877 days. cf., Fig 52.

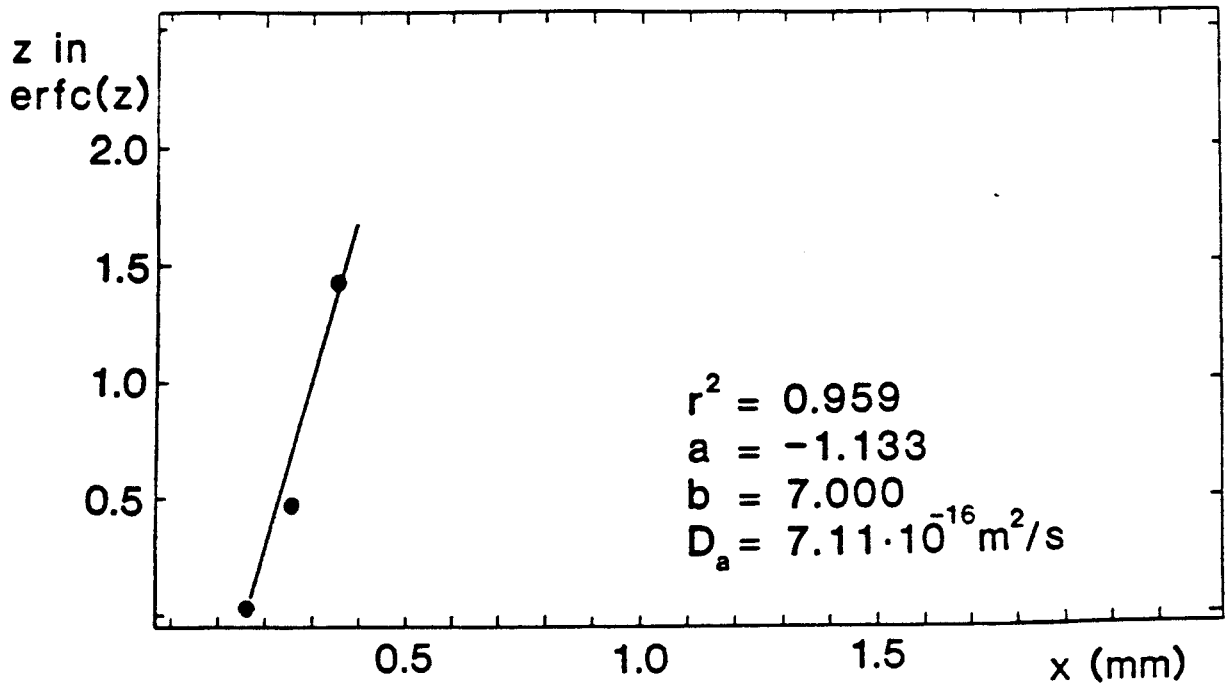


Fig 35. Diffusion of americium in Studsvik gneiss(Stu 183.1:1r)
 Diffusion time 85 days.

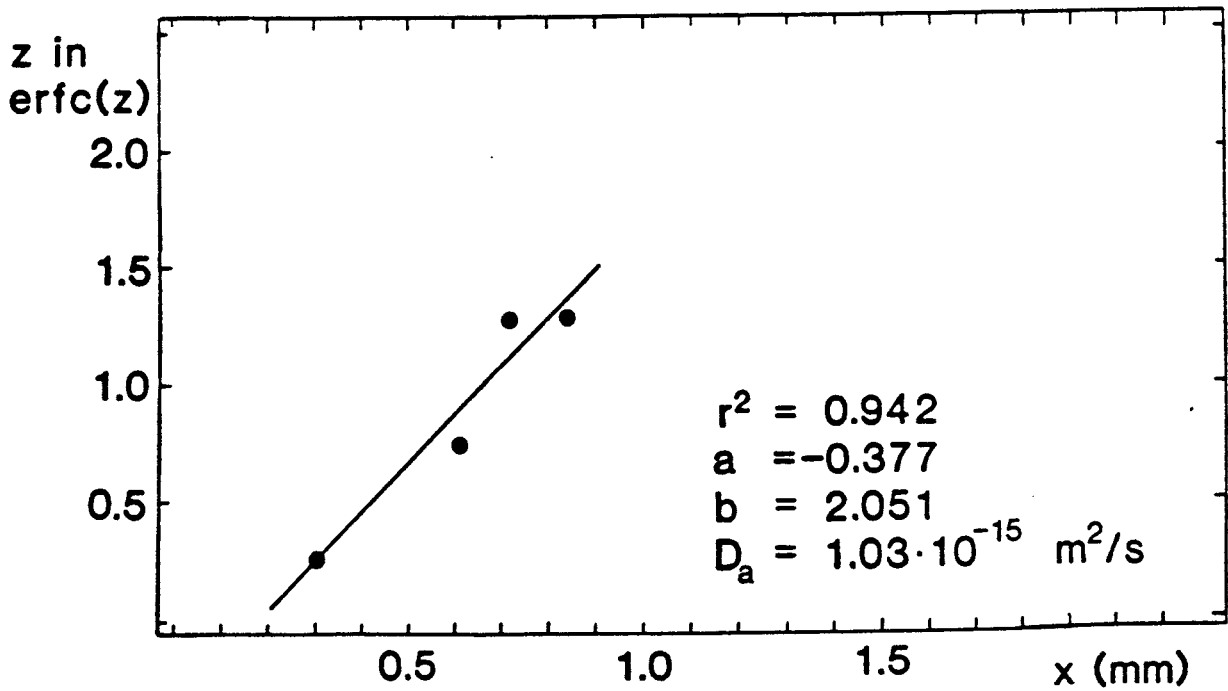


Fig 36. Diffusion of americium in Stripa granite(Str 3:1)
 Diffusion time 665 days. cf., Fig 53.

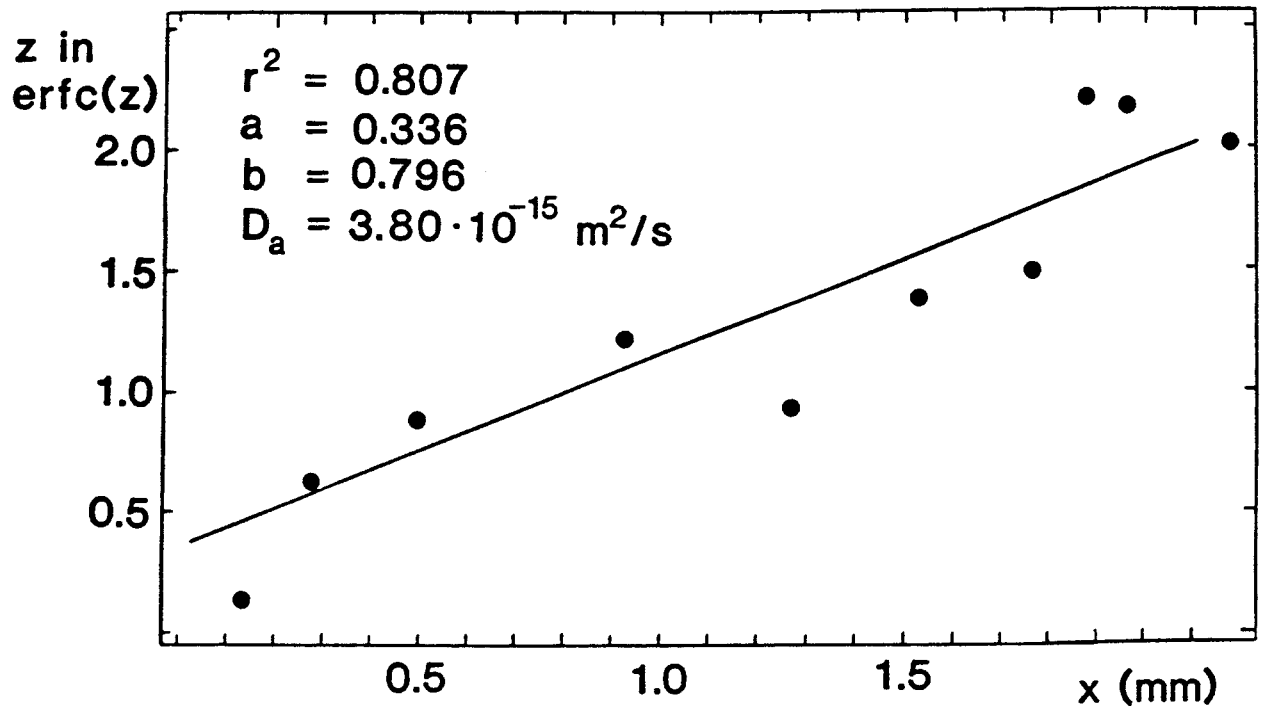


Fig 37. Diffusion of americium in Stripa granite(Str MS:3)
Diffusion time 1202 days. cf., Fig 54.

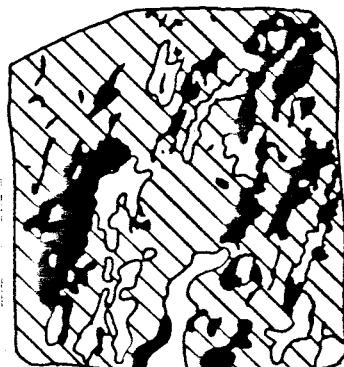
Photograph Fi7 526.5

Mineralogic composition

Autoradiograph



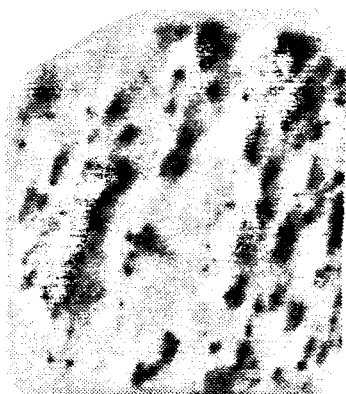
0



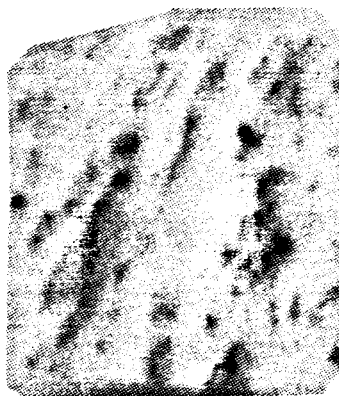
0




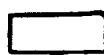



0



1.19



2.55

-  = Feldspars and minor quartz grains
-  = Major quartz grains
-  = Biotite
-  = Chlorite
-  = Garnet





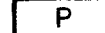
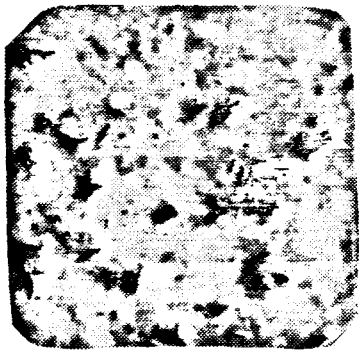
-  = Fragments of epidote, chlorite and muscovite
-  = Fragments of quartz and feldspars
-  = Calcite
-  = Laumontite
-  = Paint

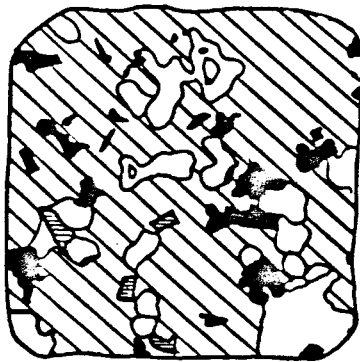
Fig 38. Autoradiographs showing diffusion of strontium in Finnsjö granite. Penetration depth are given in mm. cf., Fig 1.

Photograph Str 2:2



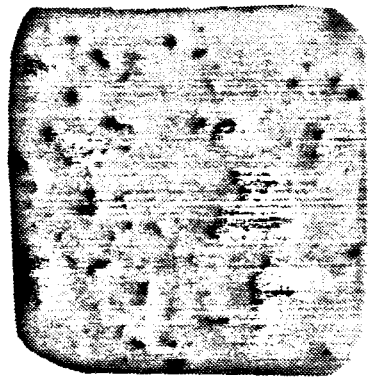
0

Mineralogic composition



0

Autoradiograph



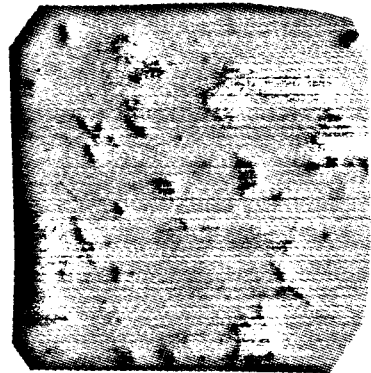
0



0.04



0.12



1.72

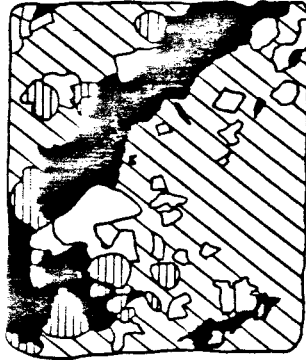
Fig 39. Autoradiographs showing diffusion of strontium in Striata granite. Penetration depth are given in mm. Key to mineralogic composition in fig 38. cf., Fig 2.

Photograph Stu 6:3



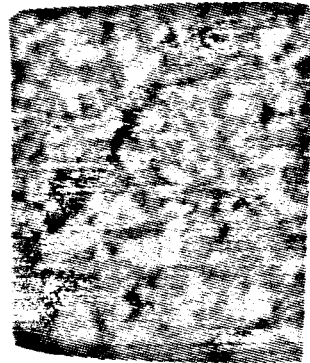
0

Mineralogic composition

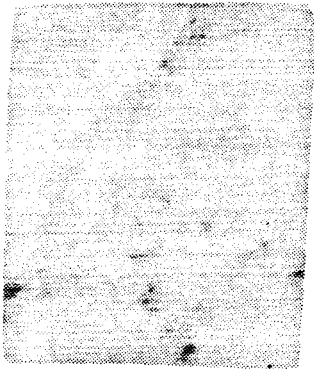


0

Autoradiograph



0



2.46

Fig 40. Autoradiographs showing diffusion of strontium in Studsvik gneiss. Penetration depth are given in mm. Key to mineralogic composition in fig 38. cf., Fig 3.

Photograph Str 2:1

Mineralogic composition

Autoradiograph



0



0



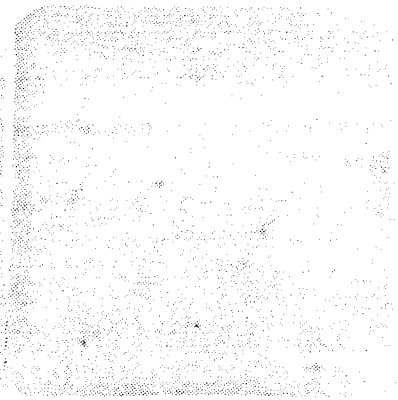
0



0.05



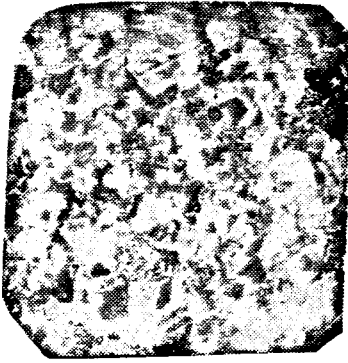
0.10



0.60

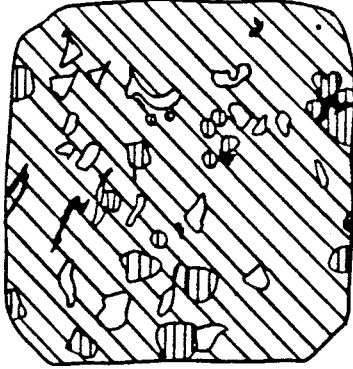
Fig 41. Autoradiographs showing diffusion of iodine in Stripa granite. Penetration depth are given in mm. Key to mineralogic composition in fig 38. cf., Fig 13.

Photograph Stu A:2



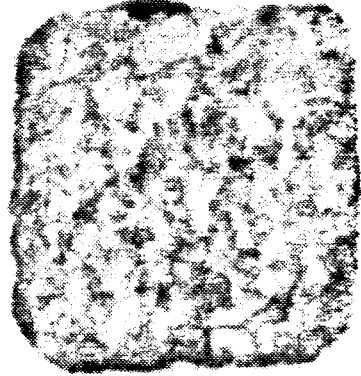
0

Mineralogic composition

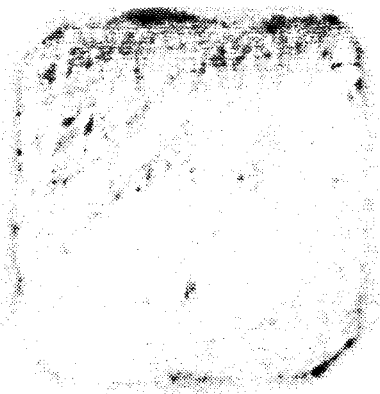


0

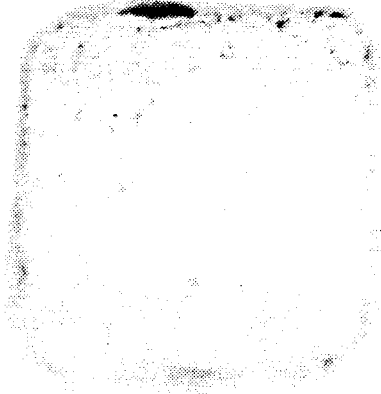
Autoradiograph



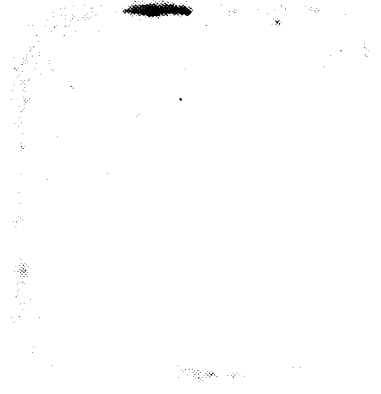
0



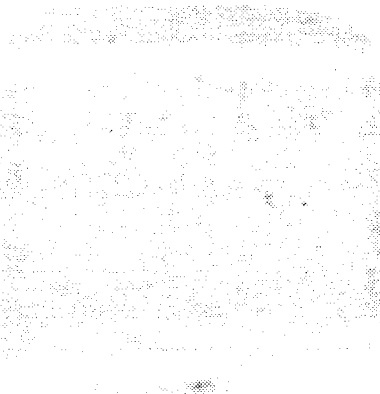
0.09



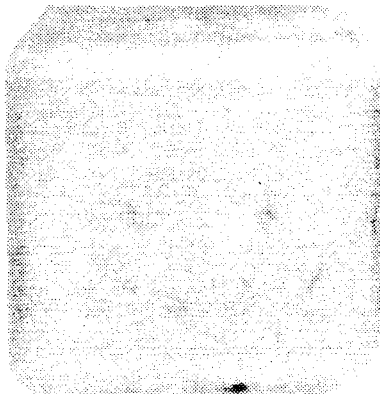
0.14



0.20



0.26



0.72

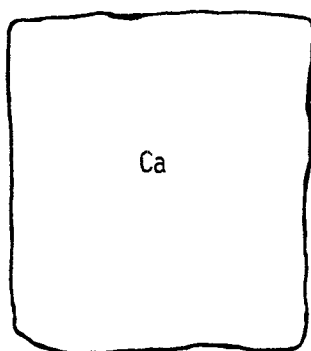
Fig 42. Autoradiographs showing diffusion of iodine in Studsvik gneiss. Penetration depth are given in mm. Key to mineralogic composition in fig 38. cf., Fig 14.

Photograph Fi6 309.0:1 Mineralogic composition

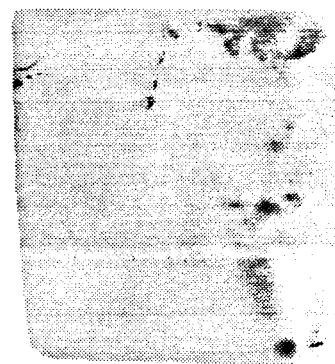
Autoradiograph



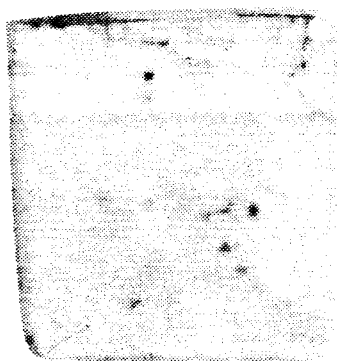
0



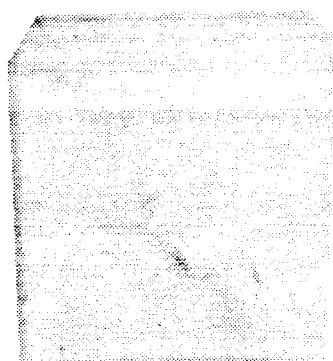
0



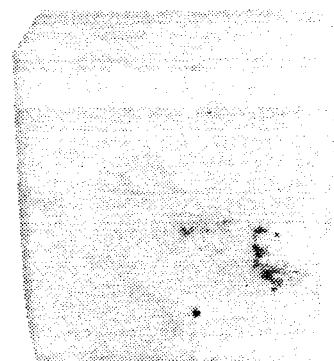
0



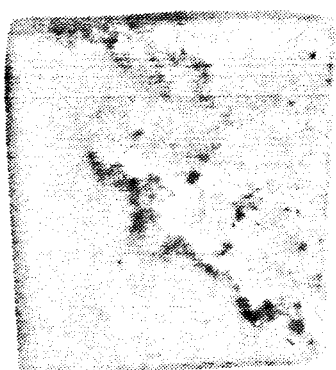
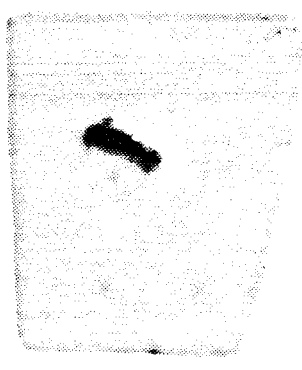
1.47



2.14



3.26

4.32
(3 x exp t)12.06
(3 x exp t)

Photograph

12.06

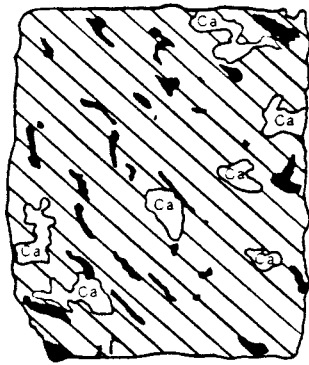
Fig 43. Autoradiographs showing diffusion of cesium in Finnsjö granite (calcite). Penetration depth are given in mm. Key to mineralogic composition in fig 38. cf., Fig 15.

Photograph Fi7 318.8:1 Mineralogic composition

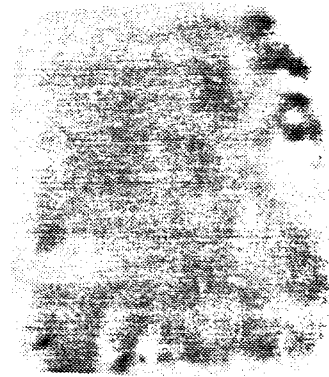
Autoradiograph



0



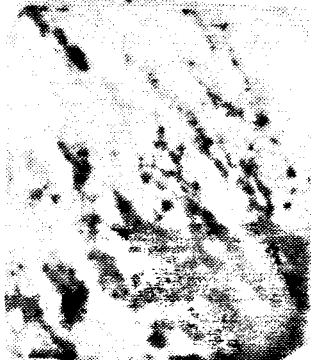
0



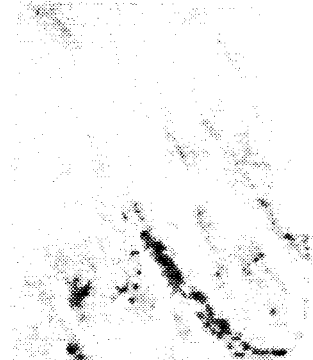
0



1.97



2.42



3.32

Fig 44. Autoradiographs showing diffusion of cesium in Finnsjö granite. Penetration depth are given in mm. Key to mineralogic composition in fig 38. cf., Fig 16.

Photograph Stu 5.4:1

Mineralogic composition

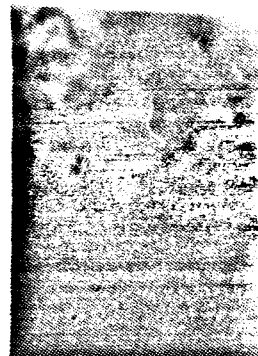
Autoradiograph



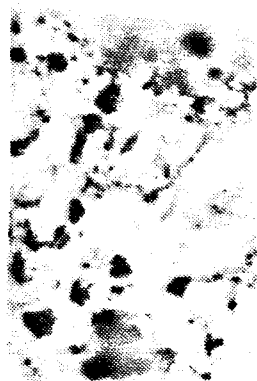
0



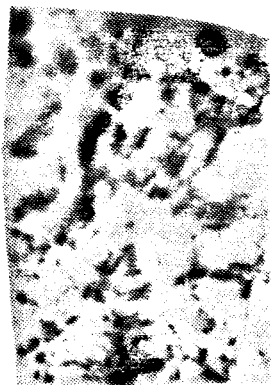
0



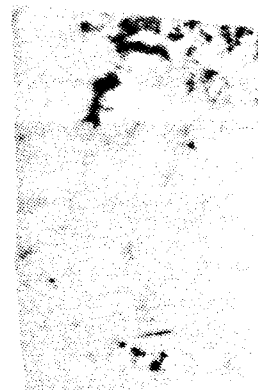
0



1.54



2.08



2.98

Fig 45. Autoradiographs showing diffusion of cesium in Studsvik gneiss. Penetration depth are given in mm. Key to mineralogic composition in fig 38. cf., Fig 20.

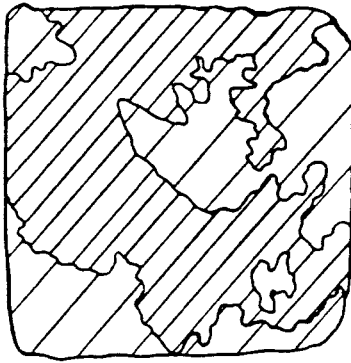
Photograph Str MS:2

Mineralogic composition

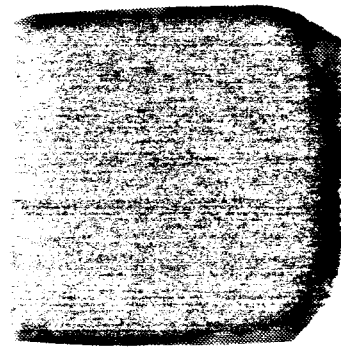
Autoradiograph



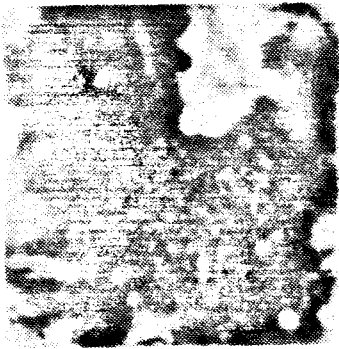
0



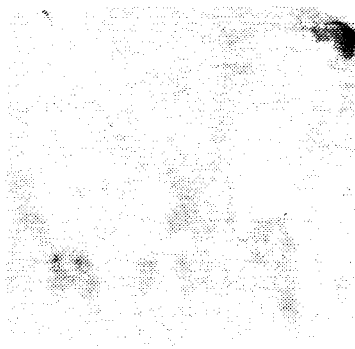
0



0



1.32



2.19

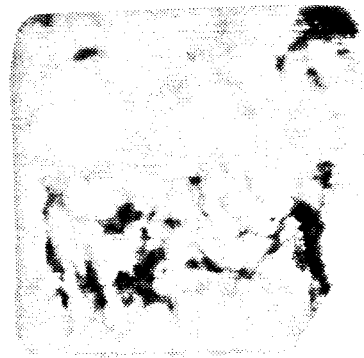
3.07
(30 x exp t)

Fig 46. Autoradiographs showing diffusion of cesium in Stripa granite. Penetration depth are given in mm. Key to mineralogic composition in fig 38. cf., Fig 25.

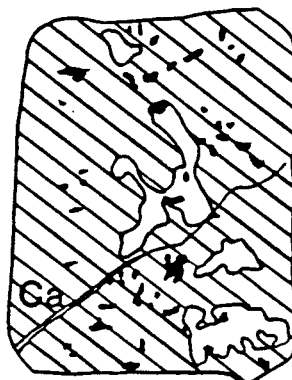
Photograph Fi8 358.1:1

Mineralogic composition

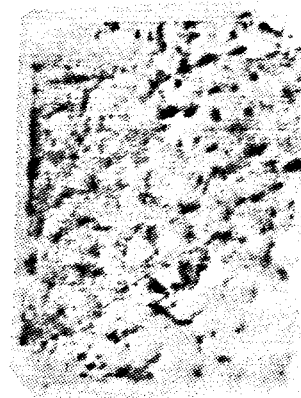
Autoradiograph



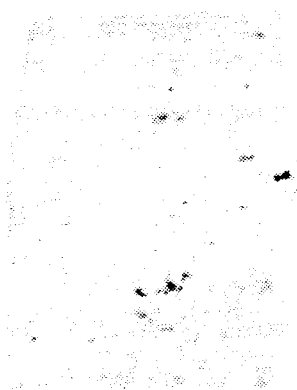
0



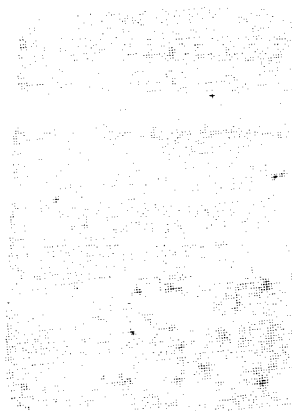
0



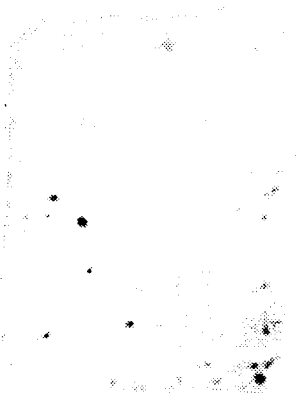
0



0.04



0.22



0.35

(4.5 x exp t)



0.74

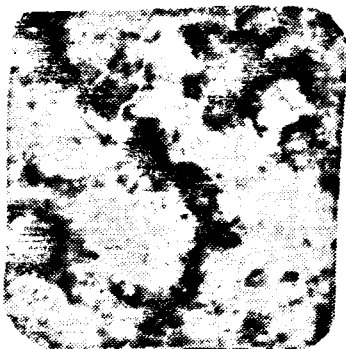
(40 x exp t)

Fig 47. Autoradiographs showing diffusion of neptunium in Finnsjö granite. Penetration depth are given in mm. Key to mineralogic composition in fig 38. cf., Fig 27.

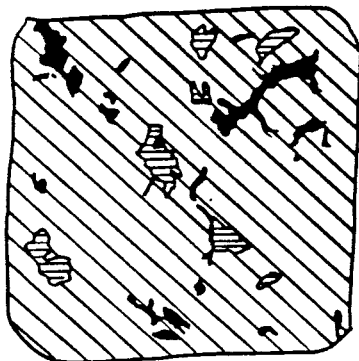
Photograph Str 3:4

Mineralogic composition

Autoradiograph



0



0



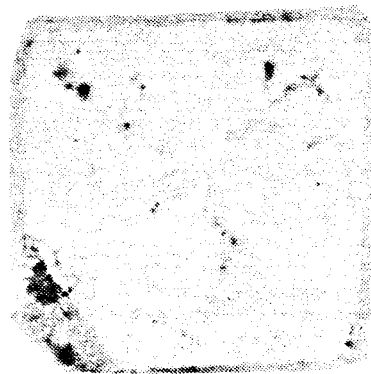
0



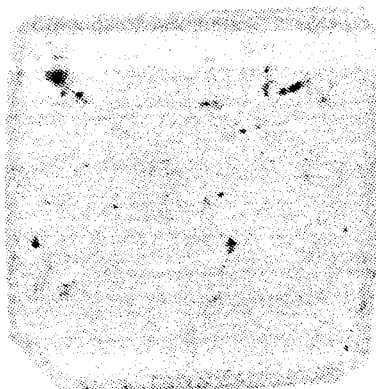
0.10



0.25



0.30



0.53

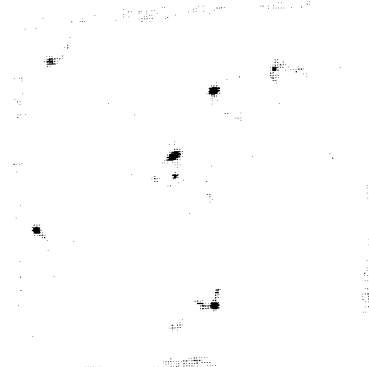
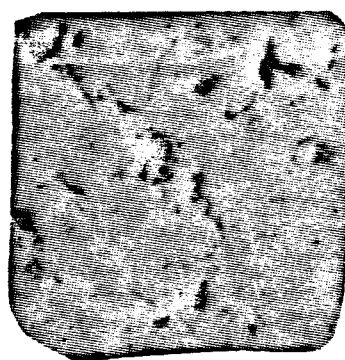
0.97
(4 x exp t)0.97
(33 x exp t)

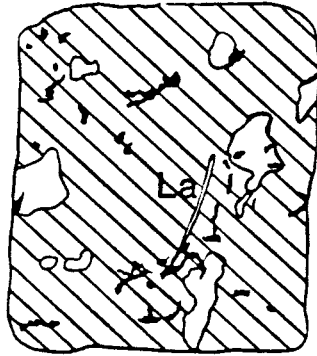
Fig 48. Autoradiographs showing diffusion of neptunium in Stripa granite. Penetration depth are given in mm. Key to mineralogical composition in fig 38. cf., Fig 28.

Photograph Fi8 358.1:2 Mineralogic composition

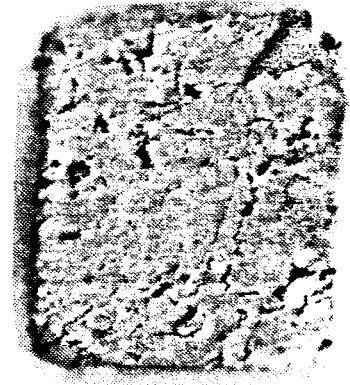
Autoradiograph



0



0



0



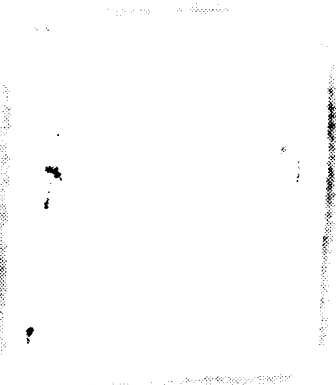
0.1



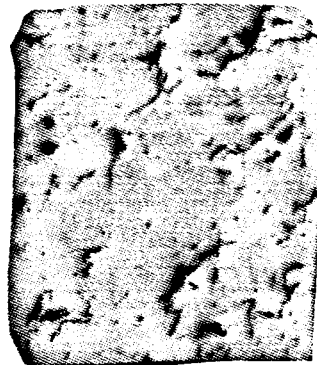
0.21



0.43



0.84



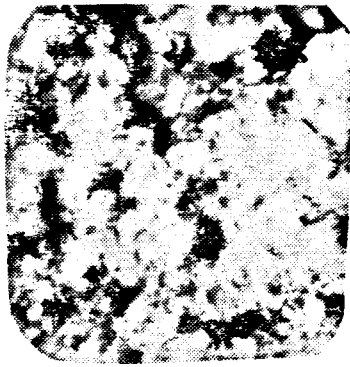
1.09
(40 x exp t)

Fig 49. Autoradiographs showing diffusion of plutonium in Finnsjö granite. Penetration depth are given in mm. Key to mineralogical composition in fig 38. cf., Fig 29.

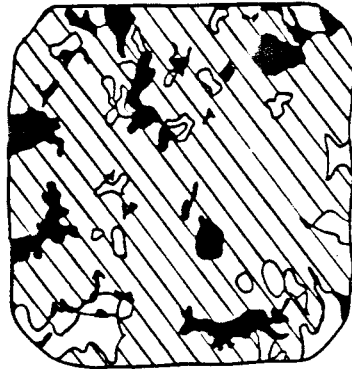
Photograph Str 4:2

Mineralogical composition

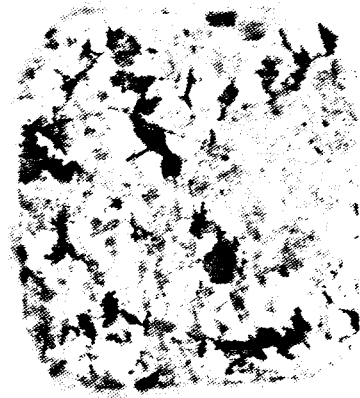
Autoradiograph



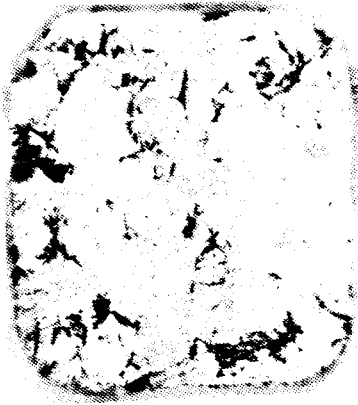
0



0



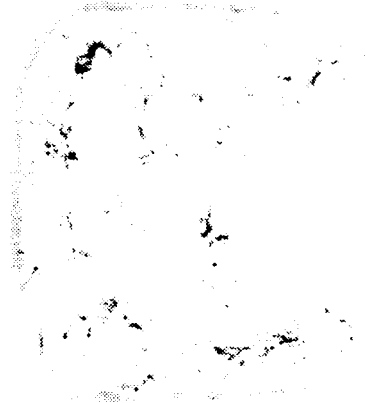
0



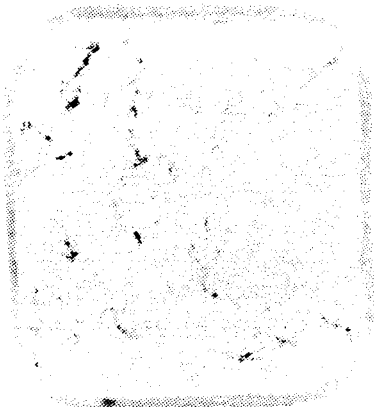
0.04



0.15



0.38



0.68

0.90
(40 x exp t)

Fig 50. Autoradiographs showing diffusion of plutonium in stripa granite. Penetration depth are given in mm. Key to mineralogical composition in fig 38. cf., Fig 30.

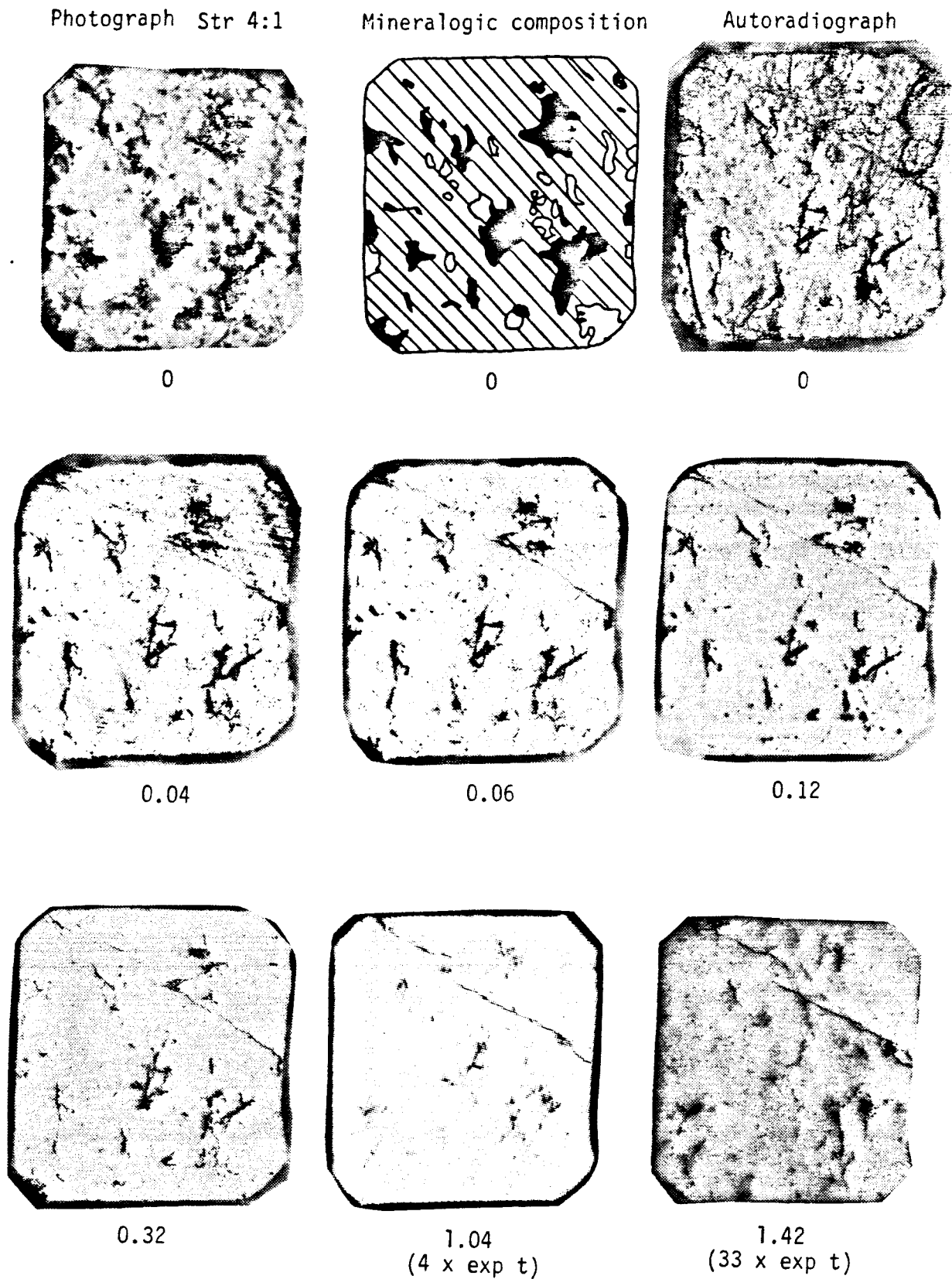
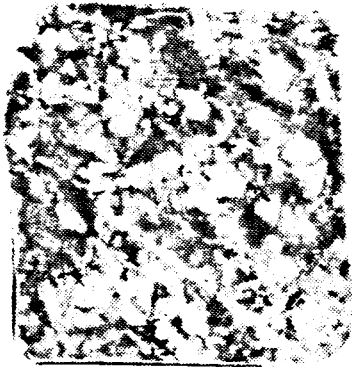


Fig 51. Autoradiographs showing diffusion of plutonium in Stripa granite. Penetration depth are given in mm. Key to mineralogical composition in fig 38. cf., Fig 31.

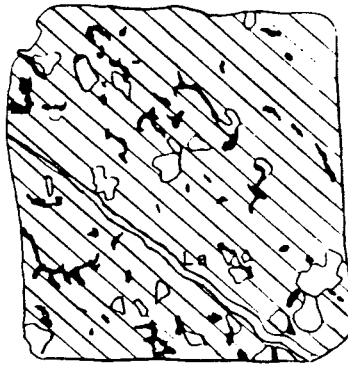
Photograph Fi8 358.1:3

Mineralogic composition

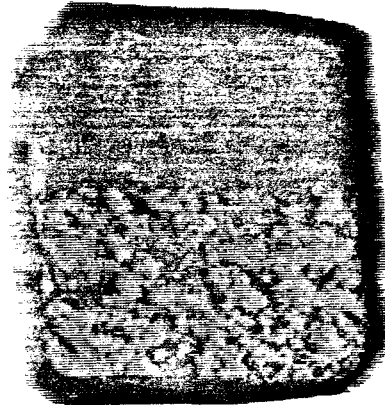
Autoradiograph



0



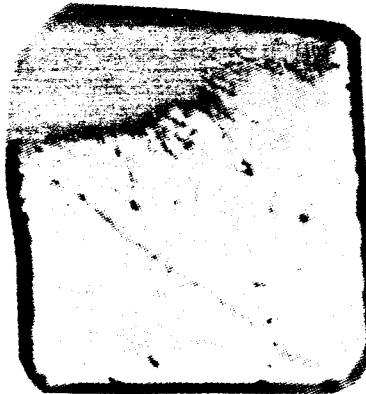
0



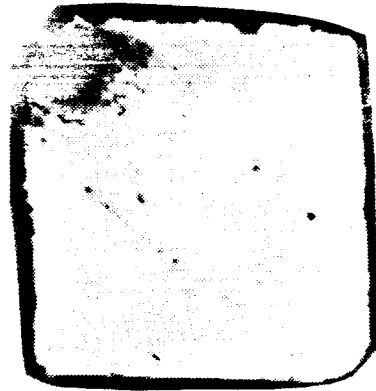
0



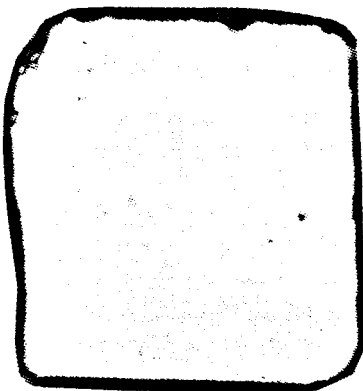
0.04



0.18



0.24



0.45

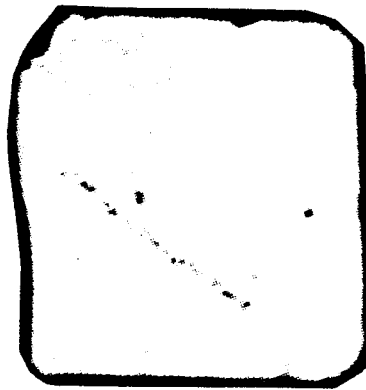
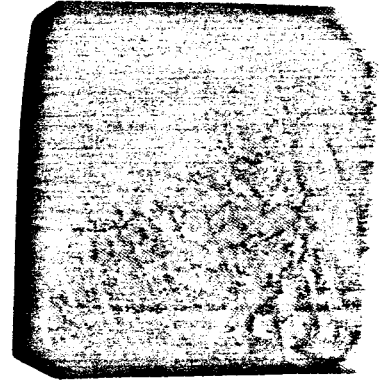
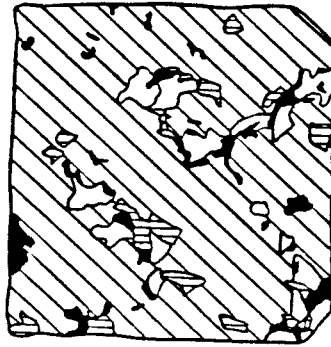
0.56
(6 x exp t)0.77
(145 x exp t)

Fig 52. Autoradiographs showing diffusion of americium in Finnsjö granite. Penetration depths are given in mm. Key to mineralogical composition in fig 38. cf., Fig 34.

Photograph Str 3:1

Mineralogic composition

Autoradiograph



0

0

0



0.01



0.07



0.14

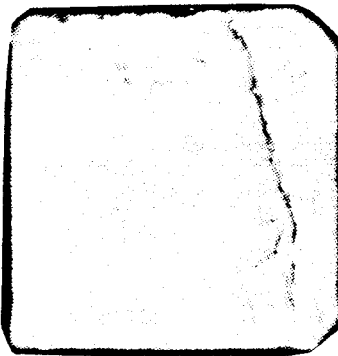
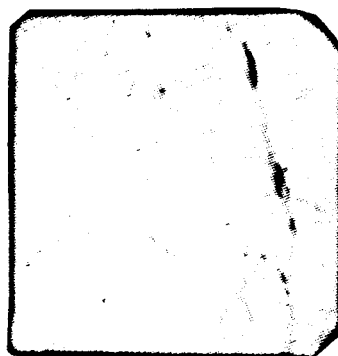
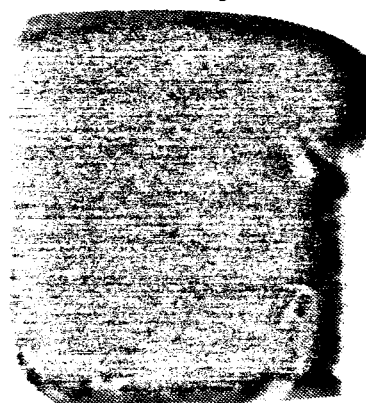
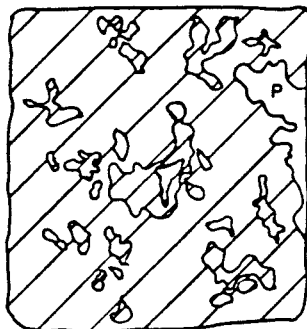
0.31
(3 x exp t)0.62
(13 x exp t)0.85
(310 x exp t)

Fig 53. Autoradiographs showing diffusion of americium in Stripa granite. Penetration depth are given in mm. Key to mineralogical composition in fig 38. cf., Fig 36.

Photograph Str MS:3

Mineralogic composition

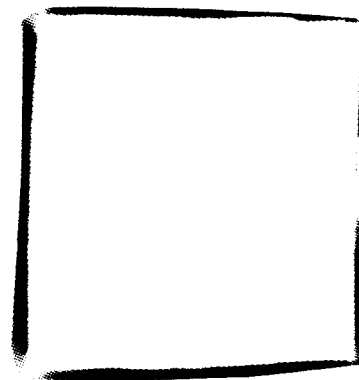
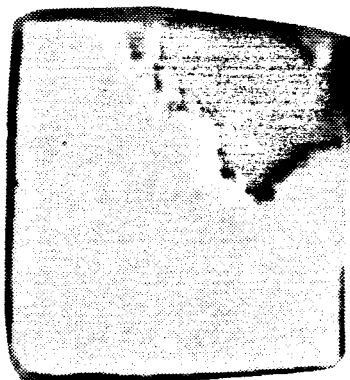
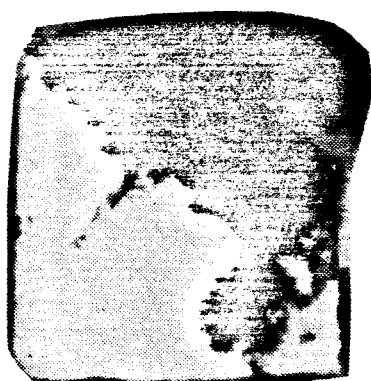
Autoradiograph



0

0

0



0.44

1.09

2.34

(4.5 x exp t)

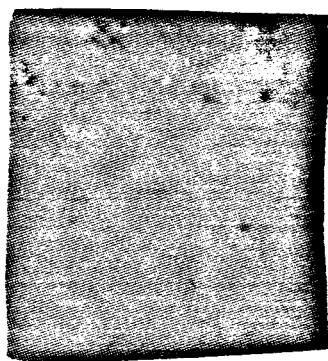
2.34
(122 x exp t)

Fig 54. Autoradiographs showing diffusion of americium in Stripa granite. Penetration depth are given in mm. Key to mineralogical composition in fig 38. cf., Fig 37.

List of SKB reports

Annual Reports

1977-78

TR 121

KBS Technical Reports 1 – 120.

Summaries. Stockholm, May 1979.

1979

TR 79-28

The KBS Annual Report 1979.

KBS Technical Reports 79-01 – 79-27.

Summaries. Stockholm, March 1980.

1980

TR 80-26

The KBS Annual Report 1980.

KBS Technical Reports 80-01 – 80-25.

Summaries. Stockholm, March 1981.

1981

TR 81-17

The KBS Annual Report 1981.

KBS Technical Reports 81-01 – 81-16.

Summaries. Stockholm, April 1982.

1982

TR 82-28

The KBS Annual Report 1982.

KBS Technical Reports 82-01 – 82-27.

Summaries. Stockholm, July 1983.

1983

TR 83-77

The KBS Annual Report 1983.

KBS Technical Reports 83-01 – 83-76

Summaries. Stockholm, June 1984.

1984

TR 85-01

Annual Research and Development Report 1984

Including Summaries of Technical Reports Issued during 1984. (Technical Reports 84-01–84-19)
Stockholm June 1985.

1985

TR 85-20

Annual Research and Development Report 1985

Including Summaries of Technical Reports Issued during 1985. (Technical Reports 85-01-85-19)
Stockholm May 1986.

1986

TR 86-31

SKB Annual Report 1986

Including Summaries of Technical Reports Issued during 1986
Stockholm, May 1987

1987

TR 87-33

SKB Annual Report 1987

Including Summaries of Technical Reports Issued during 1987
Stockholm, May 1988

Technical Reports

1988

TR 88-01

Preliminary investigations of deep groundwater microbiology in Swedish granitic

Karsten Pedersen
University of Göteborg
December 1987